



Citation for published version:

Statelova, M, Holm, R, Fotaki, N, Reppas, C & Vertzoni, M 2023, 'Usefulness of the Beagle Model in the Evaluation of Paracetamol and Ibuprofen Exposure after Oral Administration to Pediatric Populations: An Exploratory Study', *Molecular Pharmaceutics*, vol. 20, no. 6, pp. 2836-2852.
<https://doi.org/10.1021/acs.molpharmaceut.2c00926>

DOI:

[10.1021/acs.molpharmaceut.2c00926](https://doi.org/10.1021/acs.molpharmaceut.2c00926)

Publication date:

2023

Document Version

Peer reviewed version

[Link to publication](#)

This document is the Accepted Manuscript version of a Published Work that appeared in final form in *Molecular Pharmaceutics*, copyright © 2023 American Chemical Society after peer review and technical editing by the publisher. To access the final edited and published work see <https://pubs.acs.org/doi/10.1021/acs.molpharmaceut.2c00926>

University of Bath

Alternative formats

If you require this document in an alternative format, please contact:
openaccess@bath.ac.uk

General rights

Copyright and moral rights for the publications made accessible in the public portal are retained by the authors and/or other copyright owners and it is a condition of accessing publications that users recognise and abide by the legal requirements associated with these rights.

Take down policy

If you believe that this document breaches copyright please contact us providing details, and we will remove access to the work immediately and investigate your claim.

Usefulness of the beagle model in the evaluation of paracetamol and ibuprofen exposure after oral administration to paediatric populations: An exploratory study

Marina Statelova^{1,2}, René Holm^{3,4}, Nikoletta Fotaki⁵, Christos Reppas¹, Maria Vertzoni^{1*}

¹ Department of Pharmacy, National and Kapodistrian University of Athens, Athens, Greece

² Present affiliation: ARD Dissolution & Biopharmaceutics, Novartis Pharma AG, Basel, Switzerland

³ Drug Product Development, Janssen Research and Development, Johnson & Johnson, Beerse, Belgium

⁴ Department of Physics, Chemistry and Pharmacy, University of Southern Denmark, 5230 Odense, Denmark

⁵ Department of Pharmacy and Pharmacology, University of Bath, Bath, UK

* Correspondence to:

Dr Maria Vertzoni

Department of Pharmacy

National and Kapodistrian University of Athens,

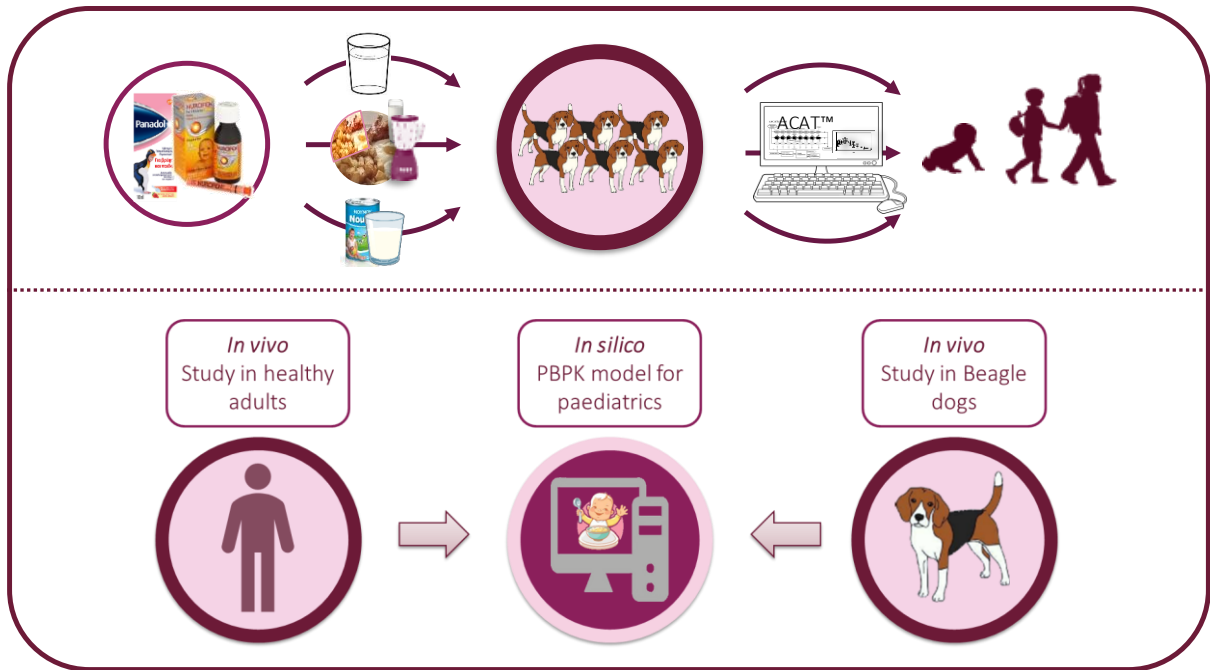
Panepistimiopolis,

157 84 Zografou, Greece

Tel. +30 210 727 4445

E-mail: vertzoni@pharm.uoa.gr

1 Graphical abstract



2

3

4 Abstract

5 The present study aimed to explore the usefulness of Beagle dogs in combination with physiologically
6 based pharmacokinetic (PBPK) modelling in the evaluation of drug exposure after oral administration
7 to paediatric populations at an early stage of pharmaceutical product development. An exploratory,
8 single-dose, crossover bioavailability study in six beagles was performed. A paracetamol suspension
9 and an ibuprofen suspension were co-administered in the fasted state conditions, under reference-
10 meal fed state conditions, and under infant-formula fed state conditions. PBPK models developed with
11 GastroPlus v9.7 were used to inform the extrapolation of beagle data to human infants and children.
12 Beagle-based simulation outcomes were compared with published human-adult-based simulations.
13 For paracetamol, fasted state conditions and reference-meal fed state conditions in beagles appeared
14 to provide adequate information for the applied scaling approach. Fasted state and/or reference-meal
15 fed state conditions in beagles appeared suitable to simulate the performance of ibuprofen
16 suspension to paediatric populations. Contrary to human-adult-based translations, extrapolations
17 based on beagle-data collected under infant-formula fed state conditions appeared less useful for
18 informing simulations of plasma levels in paediatric populations. Beagle data collected under fasted
19 and/or reference-meal fed state conditions appeared to be useful in the investigation of paediatric
20 product performance of the two investigated highly permeable and highly soluble drugs in the upper
21 small intestine. The suitability of the beagle as a pre-clinical model to understand paediatric drug
22 product performance under different dosing conditions deserves further evaluation with broader
23 spectrum of drugs and drug products and comparisons with paediatric *in vivo* data.

24

25

26 Keywords (max. 10)

27 Food effect; Paediatrics; Beagle bioavailability study; Physiologically based Pharmacokinetic (PBPK)
28 model; Paracetamol; Ibuprofen; Infant formula; Extrapolation to paediatric populations

29

30

31 Introduction

32

33 Although paediatric drug development and drug product evaluation has advanced over the recent
34 years (1), age-appropriate tools and methodologies to predict formulation performance in paediatric
35 populations are yet to be established. Doubtlessly paediatric drug product evaluation in the target
36 population would be ideal to ensure safety and efficacy after administration to this vulnerable patient
37 group, however, ethical and recruitment issues limit investigations in paediatrics. Therefore, data from
38 bioavailability studies in adults are often extrapolated to the paediatric population of interest (1–3).
39 In line, a recent draft guideline from the U.S. Food and Drug Administration (FDA) suggested that the
40 sponsor should perform a food effect study in adults with the paediatric formulation and that “the
41 sponsor can use foods and quantities of food that are commonly consumed with drugs in a particular
42 pediatric population (e.g., formula for infants)” (4). Recent literature review highlighted the different
43 food effect observations between studies performed in healthy adult volunteers in comparison to
44 food effects observed in infants/young children who were administered the same drug (2,5). The
45 discrepancy in the food effect outcomes could be attributed to several factors: age-dependent
46 physiology differences, inconsistent protocols between adult and paediatric food effect studies, age-
47 appropriate meal chosen for each study population (standard breakfast in adults and milk-based meal
48 in paediatric populations) (2,5,6). A dedicated investigation of the factors affecting oral absorption of
49 paediatric formulations in the presence of standard solid-liquid meal or infant milk-based feed in adult
50 healthy volunteers revealed that food effects for infant formulations might not be adequately
51 evaluated when applying common adult FE study protocols (5).

52 Furthermore, as paediatric product development usually commences during the clinical stages of adult
53 drug product development, paediatric formulation development and the food effect evaluation are
54 mainly guided by the knowledge gained throughout adult formulation investigations and the relevant
55 applied protocols for adults (1,4,7,8). Within the recent FDA guidance, it is indicated that paediatric
56 product development builds upon knowledge of the adult formulation performance, i.e., when the
57 same to-be-marketed formulation that is approved for use in adults is approved for use in a pediatric
58 population, a separate FE study is not necessary (4). However, before addressing this research
59 question in the clinical setting in humans using the paediatric formulation, investigation of possible
60 food effects with age-relevant meals and quantities at a preclinical level (e.g., in Beagle dogs) could
61 de-risk paediatric formulation testing in clinic and reduce associated costs. Throughout adult drug
62 product development, food effect evaluation in the preclinical stage is commonly supported by *in vitro*
63 tools, pre-clinical animal models, and/or *in silico* tools (9,10) and has resulted in a confirmatory rather
64 than exploratory nature of the clinical food effect studies for adult products (11–13). In paediatrics,

65 considering the limitations surrounding the establishment of validated age-appropriate *in vitro* and
66 *in silico* tools to be used as standalone methodologies for predicting product performance prior to
67 testing in human (7); adaptation of existing study protocols for animal models, as the beagle, could
68 offer additional insights to understand oral dosage behavior, especially regarding mechanical/physical
69 interactions between drug components/food components.

70 Based on the similarities between the canine and human adult gastrointestinal (GI) tract and the
71 relatively easy handling of the breed, preclinical bioavailability/food effect studies are often
72 performed in beagles (14–17). Despite several similarities, differences in GI anatomy and physiology
73 between humans and beagles may increase the complexity of directly translating preclinical outcomes
74 into human, e.g., basal gastric secretions, pH of fluids along segments of the GI tract, intraluminal bile
75 salt composition and levels, transit times, and intestinal permeability (17). A major difference between
76 beagles and human adults that might affect performance of ionizable, poorly soluble drugs is the lower
77 level of basal gastric secretions in beagles that could lead to elevated fasted gastric pH in the fasted
78 state and greater variability of intragastric pH compared to human adults (14,15,18,19). In an effort
79 to overcome this interspecies difference when investigating formulations for humans and to control
80 intragastric pH, oral administration of HCl/KCl solution prior to drug dosing has been demonstrated to
81 induce acidic environment in the canine stomach with an acceptable reproducibility (18).

82 In addition to the disparities between human and canine GI physiology that control drug absorption,
83 interspecies differences in disposition, metabolism, and elimination further complicated efforts for
84 direct results extrapolation from bioavailability/food effect studies from beagles to human adults (10).
85 Mechanistic approaches, such as physiologically based pharmacokinetic (PBPK) modeling have been
86 utilized to account for these differences and translate relevant biopharmaceutical information from
87 canine studies into the human adult model; furthermore, the preclinical model has been used to
88 identify sensitive parameters regarding oral drug/drug product performance in adults (20–23).

89 Furthermore, the dog model has been suggested to be potentially useful for paediatric formulation
90 testing based on its role in adult drug product development (7). To date, only few relevant studies
91 have been reported in the preclinical species and the evaluation of their usefulness has been limited
92 due to lack of paediatric clinical data to serve as confirmatory dataset (7). The elevated bile salt levels
93 in dogs have been mentioned as one factor that complicates results interpretation (7).

94 The aim of this study was to explore the usefulness of the beagle model in the evaluation of drug
95 exposure after oral administration to paediatric populations and compare it with the human adult
96 model. In line with the design of the human adult bioavailability data acquired under different dosing

97 conditions (5), the first objective was to design comparative bioavailability studies of two paediatric
98 drug products under different prandial and dosing conditions, i.e.,

- 99 • fasted state conditions
- 100 • fasted state conditions with gastric pH-lowering pretreatment
- 101 • reference-meal fed state conditions
- 102 • dosing conditions simulating the infant-formula fed state conditions.

103

104 The second objective was to propose a PBPK approach for modeling the collected data and investigate
105 if the conditions applied to beagles substantially affected extrapolation to paediatric populations. The
106 third objective was to compare the usefulness of the beagle data in evaluating drug exposure in
107 paediatric populations with the respective translation based on human adults (24,25).

108 Paracetamol (high solubility, weak acid, pka 9.5, BCS Class I) and ibuprofen (low solubility, weak acid,
109 pka 4.5, BCS Class II) (26–28) were selected as model drugs based on their luminal stability and high
110 intestinal permeability, as in the respective investigations in adults (5,24,25). Additionally, based on
111 their physicochemical properties, both drugs are expected to be highly soluble in the upper small
112 intestine. After confirming the lack of pharmaceutical and pharmacokinetic interaction (29,30), the
113 drugs were co-administered using the commercially available paediatric suspensions, i.e., variations
114 of dosing should impact primarily gastric emptying (paracetamol) or gastric emptying and, perhaps,
115 dissolution (ibuprofen).

116

117 Materials and methods

118 Materials

119 The paracetamol solution for intravenous (i.v.) administration was prepared in-house by dissolving
120 paracetamol powder in saline for i.v. use with a final concentration of 10 mg/mL (Esco, European salt
121 company GmbH & Co. KG, Germany). The ibuprofen solution for i.v. administration (5 mg/mL) was
122 prepared in-house by dissolving ibuprofen in 50 mM Tris solution under addition of NaCl
123 (876 mg/100 mL) to reach isotonicity, followed by pH adjustment to 7.6 with 1 M HCl. Both solutions
124 were filtered through a 0.22 µm Millex®-GV PVDF filter. Nurofen® paediatric suspension with 100 mg
125 ibuprofen/5 mL (Reckitt Benckiser UK Ltd., Berkshire, UK) and Panadol® paediatric suspension with
126 120 mg paracetamol/5mL (GlaxoSmithKline A.E.B.E., Middlesex, UK) were acquired from a local
127 pharmacy in Athens, Greece.

128 Food products for the reference meal were supplied from a local supermarket. The reference meal
129 consisted of two slices of toasted bread with butter, two strips of bacon fried in butter, two eggs fried
130 in butter, French fries, and a glass of full-fat cow's milk; this resulted in 67 g of fat, 63 g of
131 carbohydrates, 36 g of protein (60 % fat, 25 % carbohydrates, 15 % proteins) according to the
132 recommended meal by regulators (4,31). The reference meal was prepared in a similar manner to a
133 recently reported clinical study in adults (5) and was cooked in the evening prior to the relevant study
134 day. On the study day, the meal was homogenized, and a portion of 100 g (200 kcal) was administered
135 to each dog via gavage. Infant formula milk (Noulac® for infants) was used as in the clinical study (5).
136 The infant formula was prepared according to instructions in the morning of the study day. The
137 administered volume per dog was 150 mL (100 kcal) and it consisted of 43 % fats, 47 % carbohydrates,
138 and 10 % proteins.

139 Acetonitrile and water (MilliQ®-System, Merck KGaA, Darmstadt, Germany) were of LC-MS/MS grade,
140 trifluoroacetic acid (TFA, 99.5 % w/w) was of protein sequencing grade, HCl (1.0 M) and KCl were of
141 analytical grade. All chemicals were supplied from Merck KGaA (Darmstadt, Germany).

142

143 Methods

144 Study in beagle dogs

145 The animal study described in this work was performed according to current relevant European
146 directive on protection of animals used for scientific purposes (2010/63/EU) and Belgian law
147 regulating Animal Welfare of test animals (<https://www.lne.be/proefdierlabo>). The study protocol

148 was approved by the institutional Ethics Committee of Janssen Pharmaceutica, Belgium (approval nr.
149 512).

150 Six healthy male beagles from the in-house colony (supplied from Marshall[®] colony, Marshall
151 BioResources, Lyon, France) aged between 1.7-4.0 years (mean 2.17) and weighing 7.9-13.3 kg
152 (mean 10.3) were included in this study. The dogs had unrestricted access to water throughout the
153 study. On study days, animals were placed and kept individually for four hours after dosing, after
154 which period the dogs were returned to their daily routine. On non-experimental days, the dogs
155 received their portion of canine dry pellets (LabDiet[®], St. Louis, Mo, USA) once daily at noon.

156

157 *Experimental protocol*

158 This single-dose bioavailability study was performed on a crossover basis following a block design. Six
159 treatments were applied on separate occasions within the study and are listed in Table I. Drug doses
160 and meal quantities were scaled based on the mean body weight (BW) of the healthy adults in a
161 human relative bioavailability study performed with the same drug formulations under different
162 dosing conditions (≈ 76 kg) (4,24) and a typical BW of a beagle ≈ 13 kg (14,19,32). A single dose of
163 168 mg paracetamol and 140 mg of ibuprofen per dog were administered in all six study phases. In
164 Phases 1 and 2, paracetamol (168 mg per dog) or ibuprofen (140 mg per dog) were administered
165 intravenously on two separate study days. In the other four study phases the two drugs were co-
166 administered orally as their respective paediatric suspensions, i.e., 7 mL Panadol[®]
167 (168 mg paracetamol) and 7 mL Nurofen[®] (140 mg ibuprofen). Each study phase was separated by a
168 recovery/wash-out period of at least six days.

169 Intravenous drug administrations (Phases 1 and 2, Table I) were performed in the fasted state and
170 drugs were administered as single bolus injection into the cephalic vein. Oral administrations in the
171 fasted state were performed in Phases 3 and 4, as shown in Table . Several reports have indicated
172 elevated pH levels in the canine stomach and high variability in gastric pH values between
173 dogs (18,19,33,34). To evaluate the importance of this difference between beagles and humans, drug
174 exposure in the fasted state was evaluated with and without administration of 20 mL of 0.1 M HCl/KCl
175 oral solution with pH 1.6 prior to drug dosing (18).

176 Oral administrations in the fed state was performed in Phases 5 and 6. Based on BW-scaling, 100 g
177 portion of reference meal (4,24), i.e. 200 kcal, was administered to dogs “reference-meal fed state
178 conditions” (Phase 5). The scaling was based on a meal amount of 550 g and the above mentioned BW
179 for human adults and beagle dogs, resulting in 92 g of reference meal to be administered per dog – in

180 the present study the meal mass was rounded to 100 g to improve dosing feasibility in a preclinical
 181 setting. The meal was homogenized prior to dosing to enable administration via gavage. The two
 182 paediatric suspensions were co-administered within 10 minutes after ingestion of the homogenized
 183 meal (200 kcal). As for the reference meal, the volume of infant formula to be administered per dog
 184 was based on BW-scaling using the volume administered in the human relative BA study (4,24) and
 185 the above mentioned body weights. The resulting 138 mL of infant formula were rounded to improve
 186 drug performance feasibility. In the present dog PK study, 150 mL of infant formula (100 kcal) were
 187 administered to each dog to induce “infant-formula fed state conditions” within Phase 6. The two
 188 paediatric suspensions were dosed halfway through infant formula administration (Table I).

189 **Table I** Overview of dosing conditions applied in the canine study.

Phase	Time (hh: mm, a.m.)	Dosing conditions
Intravenous bolus – fasted state		
1	08:30	16.8 mL paracetamol solution (10 mg/mL, 168 mg of paracetamol)
2	08:30	28 mL ibuprofen solution (5 mg/mL, 140 mg ibuprofen).
Per os administration ^a – fasted state conditions		
3	08:30	7 mL Panadol [®] suspension ^b and 7 mL Nurofen [®] suspension ^c , followed by tube rinse with 10 mL of tap water.
4	08:20 08:30	20 mL 0.1 M HCl/KCl-solution, pH 1.6 (pH-lowering pretreatment) 7 mL Panadol [®] suspension ^b and 7 mL Nurofen [®] suspension ^c , followed by tube rinse with 10 mL of tap water.
Per os administration ^a – fed state conditions		
5	08:20 08:30	100 g homogenized reference meal (200 kcal) 7 mL Panadol [®] suspension ^b and 7 mL Nurofen [®] suspension ^c , followed by tube rinse with 10 mL of tap water.
6	08:29 08:30 08:31	75 mL infant formula (50 kcal) 7 mL Panadol [®] suspension ^b and 7 mL Nurofen [®] suspension ^c 75 mL infant formula (50 kcal)

190 ^a dosing performed via gavage

191 ^b 7 mL of Panadol[®] suspension (24 mg paracetamol/mL) contain 168 mg paracetamol

192 ^c 7 mL of Nurofen[®] suspension (20 mg ibuprofen/mL) contain 140 mg ibuprofen

193

194 Each study day was initiated in the morning after a fasting period of at least 16 hours. The dogs were
 195 guided to their individual area designated for the duration of drug dosing. A pretreatment blood
 196 sample of 2 mL was collected through venipuncture of the jugular vein. Following drug dosing, blood

197 sampling was performed at pre-defined time intervals alternating between the left and right jugular
198 veins. Blood sampling after i.v. drug administration was performed at 10, 20, 30, 45 min and 1, 2, 3, 4,
199 6, 8, and 10 h post-dose. Within study phases employing oral route of drug administration, 2-mL blood
200 samples were collected 20, 40 min, 1, 1.5, 2, 2.5, 3, 4, 5, 6, 8, and 10 h post-dose. On treatment days
201 requiring drugs administration under fasted state conditions, the dogs received the daily portion of
202 canine food pellets as usual around noon, i.e., 2.5 -3 h after drugs administration. In study phases 5
203 and 6, no further food was provided for the day. After collecting the 4-h-sample, animals could return
204 to their usual daily routine, while blood sampling continued occasionally until the end of the study
205 day.

206

207 *Sample handling and drug analysis*

208 Blood samples were collected into K₂-EDTA Vacutainer™ tubes (Becton, Dickinson U.K. Ltd., Berkshire,
209 UK) and were centrifuged for 10 minutes at 9,000 g at 5° C to obtain plasma (Centrifuge 5430 R,
210 Eppendorf AG, Germany). Plasma was transferred into amber screw cap micro tubes of 2 mL (Thermo
211 Scientific™, Waltham, MA, USA), frozen and stored at -20°C. Analysis of paracetamol and ibuprofen
212 was performed according to the methods described in Statelova et al., 2020a (5) and the
213 Supplementary information, Part A.

214

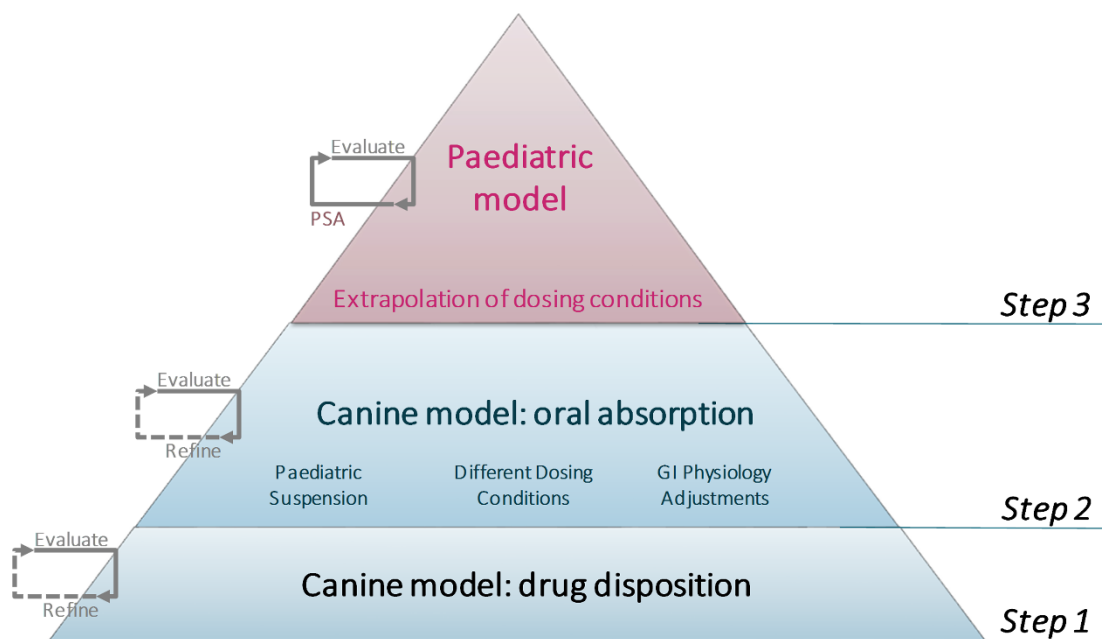
215 *Data analysis*

216 Concentrations for samples under the low limit of quantification (LLOQ) were considered as zero.
217 Individual and mean plasma concentration-time profiles were evaluated using non-compartmental
218 pharmacokinetic (PK) analysis, i.e., area under the plasma concentration-time curve up to the last
219 sampling point 0-10 h (AUC_{0-10h}), AUC_{0-inf} (extrapolated to infinity based on the first order elimination
220 rate constant estimated from the last three sampling points), maximum concentration (C_{max}), and time
221 to reach C_{max} (T_{max}). Additionally, for the study arms investigating dosing after i.v. administration,
222 additionally, clearance (CL) and volume of distribution at steady state (V_{ss}) were estimated for the
223 individual dog plasma concentration-time profiles and for the mean plasma concentration-time profile
224 (PKPlus™ tool within GastroPlus™ platform, Simulations Plus Inc.). Mean, standard deviation (SD), and
225 % relative standard deviation (RSD) values were calculated from the individual PK parameters.

226 PBPK modeling

227 *PBPK modeling workflow*

228 PBPK models were developed and refined for paracetamol and ibuprofen separately following an
229 identical modeling workflow using GastroPlus™ (Simulations Plus Inc., V9.7), Figure 1. As a first step,
230 the drug disposition model was developed based on i.v. data in beagles. As a second step, the oral
231 absorption ACAT™ model was refined for the different dosing conditions applied in the preclinical
232 study. In the third step, the different dosing conditions were extrapolated to the target paediatric
233 populations for each model drug based on previously developed and published paediatric PBPK
234 models (24,25). The paediatric simulations following oral dosing were evaluated using paediatric
235 clinical data in infants after oral paracetamol administration (35,36) and in mixed paediatric
236 populations (infants and children or children) after oral ibuprofen administration (37,38).



237

238 **Figure 1** Modeling workflow for the extrapolation of bioavailability data in beagles to paediatrics.

239

240 *Step 1: Disposition model in beagles*

241 Drug-dependent and PK parameters used for model development of paracetamol and ibuprofen are
242 reported in Table B-SIII and Table B-SIV. One and two compartment models were tested for each drug
243 with the built-in PKPlus™ tool and evaluated using the Akaike Information Criterion (AIC), Bayesian
244 Information Criterion (BIC), and the adjusted coefficient of determination (adjusted R^2). The model
245 with the lower AIC and BIC and higher adjusted coefficient of determination (R^2) was selected to
246 describe disposition, if no substantial difference between the models was found based on the model

247 evaluation criteria, the simpler model was preferred. Fraction of drug unbound and blood to plasma
248 ratio were software-proposed parameters for the respective drug. The performance of the simulations
249 was evaluated against the *in vivo* data observed in dogs and used for model development based on
250 the Average (AFE), Absolute Average fold error (AAFE), and R².

251 *Step 2: Oral absorption model in beagles*

252 ACAT™ models were used to describe oral drug absorption processes along the canine GI tract. Default
253 software parameters were used for drug mean precipitation time, particle density, and mean particle
254 radius, while diffusion coefficients were estimated from the in-built ADMET predictor within
255 GastroPlus V9.7 (Simulations Plus Inc.), reported in Table B-SIII and Table B-SIV. Drug dissolution was
256 simulated with the Johnson model. For ibuprofen, the pH versus solubility profile from literature was
257 used to fit the pKa value and solubility factor. The lowest solubility value measured within the pH
258 range 1 - 7.4 was considered as reference drug solubility (the weak acid ibuprofen is assumed to be
259 predominantly present in nonionized form at pH 1, hence, intrinsic solubility) (25,26); the pH values
260 of the buffers used for solubility determination were used as input into the pH-solubility profile. To
261 estimate the bile salt-solubilization ratio, thermodynamic solubility in buffers containing defined bile
262 salt concentrations were integrated as in human adult modeling (25), i.e., Level III fasted state
263 simulated gastric fluid (FaSSGF), Level II fasted state simulated intestinal fluid (FaSSIF), and Level II fed
264 state simulated small intestinal fluid (FeSSIF-V2). The simulations utilized the estimated bile salt-
265 solubilization ratio and accounted for diffusion coefficient adjustment in presence of bile salts.
266 Effective human permeability (Peff) values from literature in adults were converted into Peff in dogs
267 by the in-built permeability converter within GastroPlus™ (23). The default GastroPlus® Opt LogD SA/V
268 6.1 model was utilized to calculate the absorption scale factors (ASF) used for regional
269 absorption/permeability in the virtual canine physiology. This model adjusts the regional Peff based
270 on the compound partitioning at the relevant GI pH, the ionized drug amount in the GI compartment,
271 and drug lipophilicity as well as the anatomical factors of the specific compartment; ASF can have
272 direct impact on the simulated drug permeation and absorption. The default ASF model employed in
273 this study has been applied for modeling and simulation for dog models using the GastroPlus™
274 platform (23,39–42). This method of estimating ASF has been previously linked to overestimation of
275 the colonic drug absorption of lipophilic compounds due to their high logP; this potential artifact might
276 be of lesser concern for the two model drugs paracetamol and ibuprofen, as they are rapidly and
277 completely absorbed in the upper SI within the simulations.

278 Fasted state conditions with and without pH-lowering pretreatment were simulated using the “Beagle
279 fasted physiology” ACAT™ settings, while “Beagle fed physiology” ACAT™ settings were employed to

280 simulate the fed state conditions induced with the homogenized reference meal or infant formula.
 281 Relevant parameters were adjusted according to the *in vivo* observations in dogs, i.e., (i) gastric transit
 282 time (GTT) adjustment was needed to describe drug performance under fasted state conditions
 283 assuming first order gastric emptying (GE) kinetics or (ii) GTT adjustment and GE kinetics change to
 284 zero order GE to capture performance under fed state conditions induced with the homogenized
 285 reference meal and infant formula. Within the software platform, GTT for a first order GE process
 286 (fasted state conditions) represented the mean GTT described as the GE half-time ($t_{1/2}$) divided by $\ln 2$,
 287 while the GTT for a zero order GE process (fed state conditions following a homogeneous liquid)
 288 described the total GTT.

289

290 *Step 3: Extrapolation to paediatrics using PBPK modeling*

291 The paediatric models for paracetamol (24) and for ibuprofen **Error! Reference source not found.**(25)
 292 were used as basis for the present PBPK modeling exercise. The model parameters utilized for
 293 paracetamol and ibuprofen are reported in the Supplementary Information, Table B-SVI and Table B-
 294 SVIII, respectively. For simulating fasted state conditions, GTT found to best describe drug/drug
 295 product performance were inherited directly from the adjusted Beagle ACAT™ physiology.
 296 Extrapolation of drug exposure under fed state conditions was based on the typical meal types for the
 297 target age/age range, i.e., infant formula for paediatric subjects younger than 2.5 years or
 298 homogenized reference meal utilized for all age groups. To account for the age-dependent caloric
 299 content of meals and enable scaling from the beagle study to different paediatric age groups, a calorie-
 300 based normalization was performed according to Equation 1:

$$301 \quad Drug\ GTT_{paediatrics} = \frac{Meal\ caloric\ content_{paediatrics} \times Drug\ GTT_{Beagle,meal}}{Meal\ caloric\ content_{Beagle}}$$

302 Equation 1,

303 where $Drug\ GTT_{paediatrics} (h)$: the calculated GTT value to be employed within the paediatric
 304 simulation

305 $Meal\ caloric\ content_{paediatrics} (kcal)$: the recommended meal calories for the age

306 $Drug\ GTT_{Beagle,meal} (h)$: the drug GTT employed in the refined canine oral absorption model for the
 307 meal utilized, i.e. homogenized reference meal or infant formula

308 $Meal\ caloric\ content_{adults} (kcal)$: the meal calories of the meal employed in beagles, i.e. 200 kcal for
 309 the reference meal or 100 kcal for the infant formula.

310 Single simulations were performed for the mean population representatives of the available clinical
311 datasets in paediatric populations.

312 For paracetamol simulations model, a 4-month-old infant (male, 4 kg) receiving a 19.6 mg/kg dose was
313 simulated (herein, population representative), based on the mean demographic parameters from the
314 infant study including five infants (36), i.e., mean age 4 months (range 2-6 months), mean BW 4 kg
315 (2.6-6 kg). Furthermore, based on the older paediatric age group reported by Walson et al. (35), a 10-
316 month-old, 10-kg male infant virtual physiology was generated (population representative),
317 representing the mean demographic parameters reported in the paediatric study (n=12 subjects,
318 mean age 10 months, mean BW 8.6 kg). Simulations for the 10-month-old population representative
319 utilized the reported mean dose administered in this study, 12.14 mg/kg (24). For the age of 4 months
320 and 10 months, meal caloric contents of 140 kcal and 170 kcal were assumed, respectively (1,24); the
321 caloric content of the meals was based on recommended meals/portions for the specific age (1). The
322 fasted state conditions, reference-meal fed state conditions using relevant ACAT™ information from
323 the homogenized reference meal in dogs, and infant-formula fed state conditions using the relevant
324 ACAT™ information from the infant formula-fed state conditions in dogs were simulated for each
325 population representative. The simulations were compared to the mean plasma data observed in the
326 respective populations (35,36). The simulated conditions and adjusted parameters are reported in
327 Table II.

328 For the ibuprofen model, simulations for a mixed age group [infants and children, 0.3 - 12 years (38)]
329 and a children group [2 - 11 years (37)] who received 10 mg/kg ibuprofen were performed using a
330 bracketing approach (25) according to the reported age ranges in each clinical dataset. Single
331 simulations were performed for a 1-year-old (male, 10 kg), 6-year-old (male, 23 kg), and 12-year-old
332 (male, 48.5 kg); the resulting simulated mean profiles were compared to the mean profile reported in
333 the clinical dataset (38). Single simulations were performed for a 2-year-old (male, 13 kg), a 6-year-
334 old (male, 23 kg), and a 11-year-old (43.6 kg); the resulting mean simulated profiles were compared
335 to the mean reported plasma concentrations in the clinical dataset (37). Fasted state and fed state
336 ibuprofen performance adjusted according to drug performance following the homogenized
337 reference meal in beagles were simulated for all paediatric age representatives, while infant-formula
338 fed state conditions were considered for the 1- and 2-year-olds. The age-adjusted caloric contents of
339 the meals were 170 kcal, 200 kcal, 260 kcal, and 340 kcal for a 1-year-old, 2-year-old, 6-year-old, and
340 11/12-year-old, respectively. Mean simulated profiles were calculated for the (i) fasted state
341 conditions, (ii) reference-meal fed state performance, and (iii) mixed fed state conditions using infant-
342 formula-fed state performance for subjects < 2.5 years and reference-meal fed state conditions for

343 the children population representatives. The simulated conditions and simulation parameters are
344 reported in Table III.

345

346 *Model performance evaluation*

347 To compare drug exposure, the Fold Difference of simulated vs. observed ($FD_{pred/obs}$) parameters
348 were employed for AUC, C_{max} , and T_{max} values. Individual and/or mean simulated plasma
349 concentration-time profiles were compared using the average fold error (AFE) and the absolute
350 average fold error ($AAFE$) according to Eq. 2 and Eq. 3, respectively.

$$351 \quad AFE = 10^{\left(\frac{1}{n} \sum \log \left(\frac{PRED_i}{OBS_i}\right)\right)} \quad \text{Equation 2}$$

$$352 \quad AAFE = 10^{\left(\frac{1}{n} \sum \left| \log \left(\frac{PRED_i}{OBS_i}\right) \right| \right)} \quad \text{Equation 3}$$

353 where n denotes the number of observed sampling points, $PRED_i$ and OBS_i denote the simulated and
354 observed plasma concentration, respectively, at the sampling time point i.

355 To evaluate simulations in a mixed population or children populations following oral dosing of
356 ibuprofen, the mean simulated profiles and PK parameters were calculated, i.e. $FD_{pred/obs}$, AFE , and
357 $AAFE$. AFE values indicated the trend for underestimation ($AFE < 1$) or overestimation ($AFE > 1$) of
358 the observed plasma concentrations, while $AAFE$ values close to unity indicated precision of the
359 simulations. Simulations were considered adequate when $FD_{pred/obs}$ and AFE values were within two-
360 fold and $AAFE$ values were below two (43), while simulations were considered successful when
361 $FD_{pred/obs}$ and AFE fell between 0.66 - 1.5 and $AAFE$ below 1.5 (44).

362

363 *Parameter sensitivity analysis*

364 One-factor-at-a-time sensitivity analysis was performed to explore the impact of different parameters
365 within the canine model. Drug/drug product-related parameters explored were drug reference
366 solubility, particle radius, diffusion coefficient, precipitation time, and permeability. Beagle
367 physiology-relevant parameters investigated included fluid volumes and intraluminal pH in the
368 different GI compartments, GTT, small intestinal transit time, intestinal radius, length, and surface
369 area. Lastly, clinical study uncertainties were tested regarding the volume of fluid co-administered
370 with the formulation. The parameters investigated for paracetamol are reported in Table B-SV and for
371 ibuprofen in Table B-SVI. The PSA of the paediatric models has previously been performed and
372 discussed for paracetamol (24) and ibuprofen (25).

373 Results

374 Paracetamol

375 Disposition model in beagles

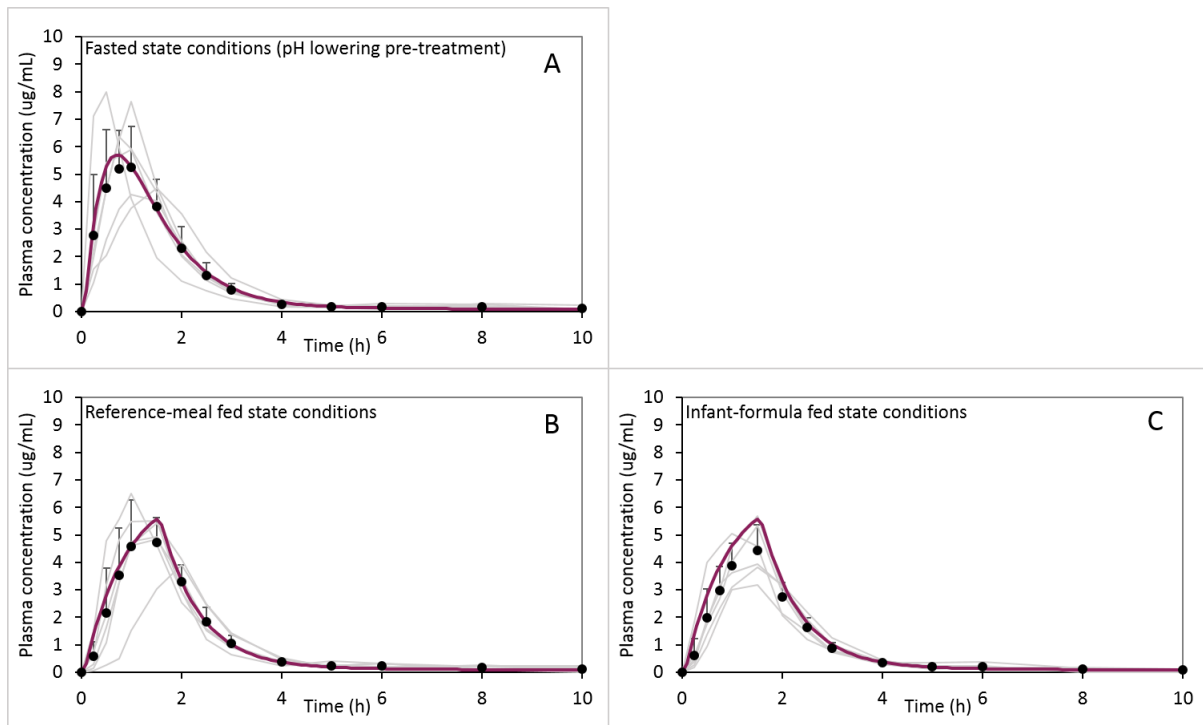
376 A two-compartment model was found to adequately describe paracetamol performance following i.v.
377 bolus administration at a dose of 168 mg per dog. The results of the compartmental PK analysis for
378 the i.v. administration performed on individual basis and for the mean profile are reported in
379 Table B-SI. Simulations performed using the developed disposition model, adequately simulated the
380 mean observed profile, as indicated by AFE 1.060, AAFE 1.104, and R^2 0.996 and shown in Figure B-S1.
381 For paracetamol the mean clearance normalized for body weight observed 1.29 ± 0.10 L/h/kg was
382 higher than in human adult subjects (0.23 - 0.335 L/h/kg), (24) or paediatrics (0.55 - 0.29 L/h/kg) (45).
383 The clearance in dogs observed in the present investigation was in line with previous investigations in
384 beagles reported in the literature (46,47). Furthermore, the estimated $f_{u,p}$ and B/P-ratios for dog were
385 similar to the ones in human, i.e., 0.82 and 1.09, respectively (Table B-SVII).

386

387 Oral absorption model in beagles

388 Oral drug absorption was simulated using the default fasted state conditions for the ACAT™ Beagle
389 physiology. GTT values were adjusted to match the observed paracetamol absorption when drug was
390 dosed following a pH-lowering pretreatment or when no pretreatment was applied. First order GE
391 kinetics and a GTT of 0.5 h were found to adequately describe both dosing conditions (Figure 2A and
392 FigureB-S2), with AAFE 1.349 and 1.195 for the fasted state conditions with and without HCl/KCl
393 pretreatment, respectively. To simulate the two fed state conditions, the ACAT™ physiology was
394 changed to “Beagle fed physiology”, zero order GE and GTT 1.5 h were employed to match the
395 observed paracetamol performance, Figure 2B and 3C.

396



397

398 **Figure 2** Observed and simulated paracetamol plasma concentration-time profiles following oral
 399 administration of 168 mg paracetamol dose (7 mL Panadol® suspension) on a crossover basis to 6 beagles
 400 applying pH-lowering pretreatment under fasted state conditions (A), under reference-meal fed state
 401 conditions (B), and infant-formula fed state conditions (C). Purple bold lines represent simulated profiles,
 402 grey lines the individual observed profiles; symbols and error bars denote observed mean concentrations
 403 and standard deviations.

404

405 [Extrapolation to infants using PBPK modeling](#)

406 A published paracetamol PBPK model was utilized for simulations of paediatric subjects; within the
 407 published PBPK model a full-body PBPK model was utilized to scale age-dependent drug disposition
 408 and enzyme-based clearance was employed to describe age-dependent clearance (24). The usefulness
 409 of the paracetamol bioavailability data obtained under different dosing conditions in beagles was
 410 evaluated using two datasets in infants who were administered paracetamol liquid formulations
 411 (35,36). To allow for the extrapolation of the fed state dosing conditions investigated in beagles to
 412 different paediatric ages, stomach transit times observed in dogs for the relevant meals were scaled
 413 on caloric basis to paediatric population representatives employing age-relevant caloric quantities for
 414 the population representatives (Eq. 1), (24).

415

416

417 **Table II** Adjusted paracetamol gastric transit time (GTT) values employing zero order gastric emptying
 418 kinetics in beagles and in infants based on meal caloric content.

Meal	Beagle dog		Infants			
	2-year-old, 10 kg body weight ^a		4-month-old, 4 kg body weight ^b		10-month-old, 9 kg body weight ^c	
	Caloric content (kcal)	GTT (h)	Caloric content (kcal)	GTT (h)	Caloric content (kcal)	GTT (h)
Reference meal	200	1.5	140	1.05	170	1.28
Infant formula	100	1.5	140	2.1	170	2.55

419 ^a mean age and body weight of male beagles (n=6)

420 ^b mean infant population representative (36)

421 ^c mean infant population representative (35)

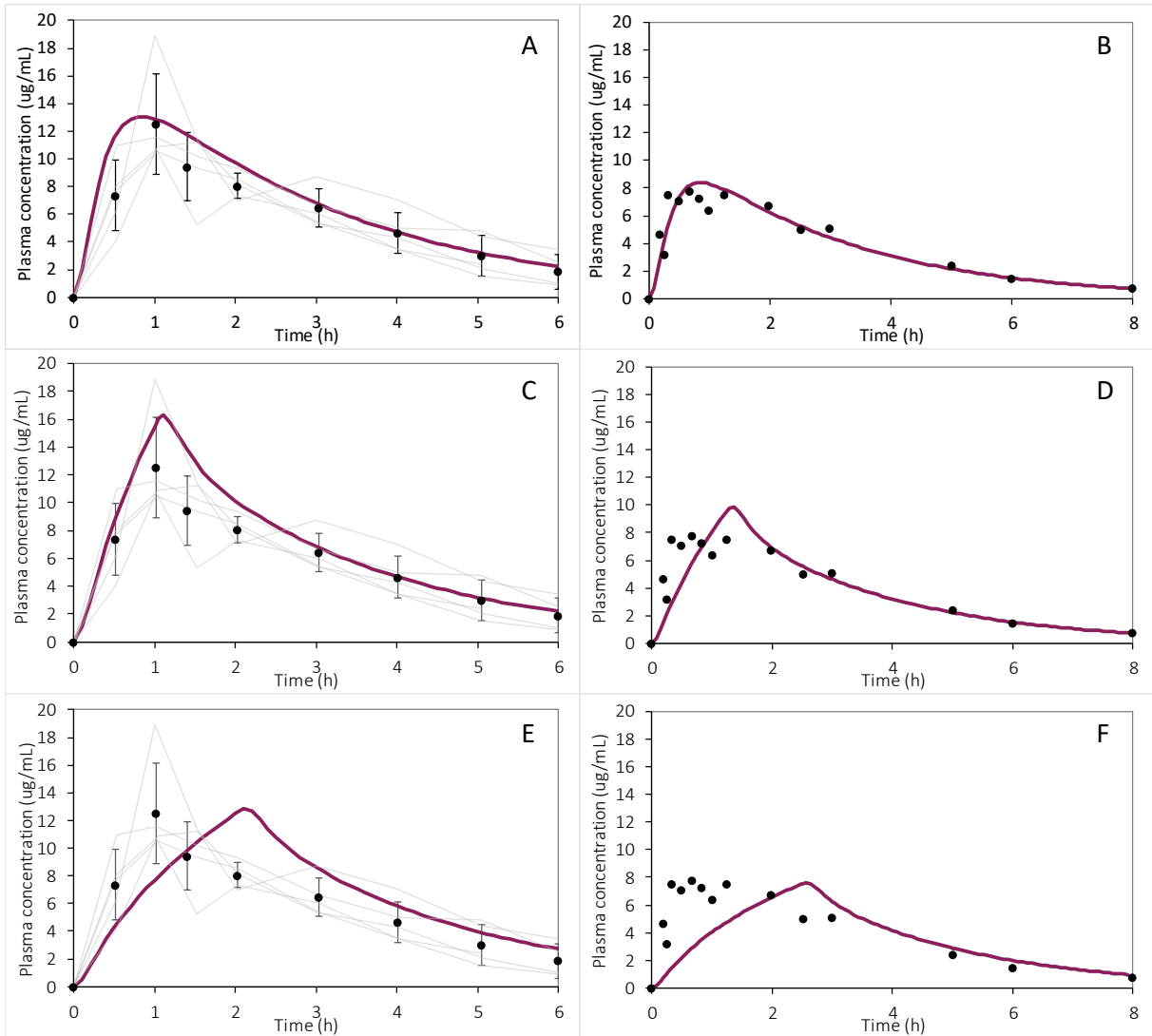
422

423 The use of fasted state GTT based on observations in beagles led to successful simulation of the 4-
 424 month-old population representative compared to observed mean data of five 2-6 month-old infants
 425 (36) and of the 10-month-old population representative compared to mean data observed in 12 3-36-
 426 month-old infants/young children (35) (Figure 3A and Figure 3B). These observations were reflected
 427 by the model evaluation metrics, Figure 4. The extrapolation based on beagle data acquired following
 428 the homogenized reference meal, resulted in a reasonable simulation of a 4-month-old population
 429 representative compared to the mean observed data in Hopkins et al. (AAFE 1.178), but led to a slight
 430 underestimation of mean plasma concentrations at early times in the 10-month-old population
 431 representative compared to the mean observed profile in the study by Walson et al. (AAFE 1.327)
 432 (Figure 3C and Figure 3D), respectively. Simulations based on paracetamol performance in beagles
 433 under infant-formula fed state conditions resulted in delayed paracetamol absorption, compared with
 434 the *in vivo* observations in infants (Figure 3E and Figure 3F). Although AAFE values and FD of AUC and
 435 C_{max} were within two-fold from the mean observations Figure 4C, T_{max} fold differences indicate the
 436 estimation mismatch, Figure 4A.

437

438

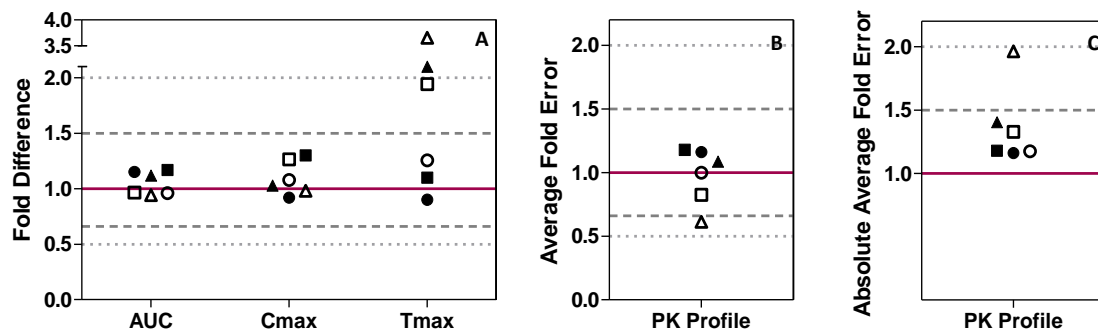
439



440

441 **Figure 3** Simulated paracetamol plasma concentration-time profiles (purple lines) based on formulation
 442 performance in beagles for a 4-month-old infant following the administration of 19.6 mg/kg dose (A, C, E)
 443 and in a 10-month-old infant following a dose of 12.14 mg/kg (B, D, F). Fasted state conditions (A, B),
 444 reference-meal fed state conditions (C, D), and infant-formula fed state conditions (E, F). Grey lines denote
 445 individual observed plasma concentration-time profiles, symbols and error bars denote mean plasma
 446 concentrations and standard deviation in 4-month-old infants (Hopkins *et al.*, 1990 (36); A, C, E); symbols
 447 denote mean plasma concentrations in 10-month-old infants (Walson *et al.*, 2013 (35); B, D, F).

448



449
 450 **Figure 4** Fold Difference (simulated/observed) for AUC_{0-8h}, C_{max}, and T_{max} (A), Average Fold Error (B), and
 451 Absolute Average Fold Error (C) for the mean profile from the study dataset from infants 2-6 months with
 452 mean age 4 months (closed symbols, Hopkins *et al.* 1990 (36)) and infants 3-36 months with mean age
 453 10 months (open symbols, Walson *et al.* 2013 (35)) under fasted state conditions (circles), reference-meal
 454 fed state conditions (squares), and infant-formula fed state conditions (triangles). The solid line represents
 455 the line of unity, grey dashed lines 0.66-1.5 range indicating successful simulations, and grey dotted lines
 456 the 0.5-2 range indicating adequate simulation.

457

458 [Parameter sensitivity analysis](#)

459 Parameters related to drug/drug product properties, physiology, and dosing conditions were
 460 investigated for the paracetamol dog PBPK model (Table B-SV). Paracetamol absorption rates were
 461 decreased by prolonged gastric transit times, indicated by the pronounced C_{max} decrease and T_{max}
 462 prolongation under all dosing conditions (Figure B-S5 and Figure B-S7). Increase in liver first pass
 463 metabolism resulted in lower total and peak exposure, as presented in Figure B-S6 and Figure B-S8. In
 464 contrast to the human PBPK models for adults and infants (24), the canine PBPK model was not greatly
 465 affected by the effective permeability value employed, with lower absorption observed firstly at 10-
 466 fold lower permeability, i.e., canine Peff 1.0 cm/s × 10⁻⁴. The canine PBPK model was overall robust
 467 and changes in the rest of the parameters tested (Table B-SV) exhibited no impact on exposure.

468 Ibuprofen

469 Disposition model in beagles

470 A one-compartment model was found to adequately describe performance of ibuprofen following i.v.
471 bolus administration at a dose of 140 mg per dog. As for paracetamol, compartmental PK analysis of
472 i.v. ibuprofen performance was performed on individual basis and for the mean profile, as shown in
473 Table B-SII. The developed disposition model was applied and adequately simulated the mean
474 observed profile in beagles, as indicated by AFE 1.060, AAFE 1.104, and R^2 0.983 and shown in
475 Figure B-S3. For the weak acid ibuprofen, the mean clearance normalized for BW observed $0.048 \pm$
476 0.005 L/h/kg was within the range of clearance reported in human adult (0.036 - 0.054 L/h/kg) and
477 paediatrics subjects (0.060 - 0.083 L/h/kg) (25). Furthermore, the estimated $f_{u,p}$ for dog was in line
478 with the high binding to plasma proteins in human plasma (human $f_{u,p}$ was 0.0155), while the
479 estimated B/P-ratio for dog (Table B-SIV) was two-fold lower than the human B/P-ratio, i.e., 1.55.

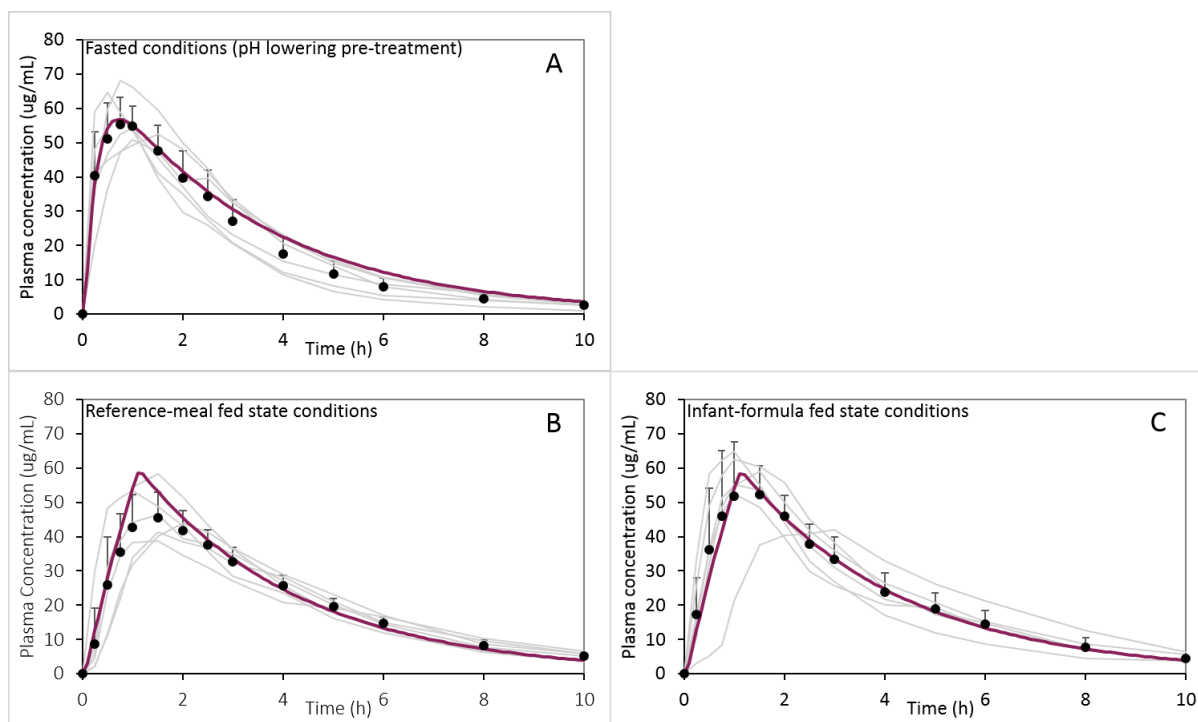
480

481 Oral absorption model in beagles

482 As for paracetamol, the fasted ACAT™ model settings were adjusted to match ibuprofen performance
483 under fasted state conditions with or without pH-lowering pretreatment. Both performances were
484 successfully simulated using the same GTT of 0.25 h for each dosing condition, i.e., AAFE 1.172 and
485 1.099 for fasted state simulations with and without the pretreatment, respectively, Figure 5A and
486 Figure B-S4. To simulate both fed state conditions, the ACAT™ physiology was changed to “Beagle fed
487 physiology” and GTT was adjusted to 1.1 h along with employing zero order GE kinetics, Figure 5B and
488 Figure 5C. Simulations of fed conditions following the administration of 200 kcal homogenized
489 reference meal and 100 kcal infant formula, were adequately described by the same ACAT™ model
490 settings with AAFE 1.144 and 1.088, respectively.

491

492



493 **Figure 5** Observed and simulated ibuprofen plasma concentration-time profiles following oral
 494 administration of 140 mg ibuprofen dose (7 mL Nurofen® suspension) on a crossover basis to 6 beagles
 495 applying pH-lowering pretreatment under fasted state conditions (A), under reference-meal fed-state
 496 conditions (B), and under infant-formula fed state conditions (C). Purple bold lines represent simulated
 497 profiles, grey lines the individual observed profiles; symbols and error bars denote observed mean
 498 concentrations and standard deviations.
 499

500

501 [Extrapolation to paediatrics using PBPK modeling](#)

502 The usefulness of the bioavailability data following ibuprofen administration under different dosing
 503 conditions in beagles was evaluated using the two most relevant, published datasets in paediatric
 504 populations, i.e., a mixed infant/children population 0.3 - 12 years (38) and a children population
 505 2 - 11 years (37), who received ibuprofen liquid formulations (37,38). To simulate fasted state
 506 formulation performance, the adjusted GTT in fasted beagles was directly inherited into the paediatric
 507 fasted state simulations. The extrapolation of the fed dosing conditions investigated in beagles to
 508 different paediatric ages was performed as for paracetamol, whereby GTT observed in dogs for the
 509 relevant meals were scaled on caloric basis to the paediatric population representative employing age-
 510 relevant caloric quantities for the population representatives (Equation 1), Table III. Mean simulated
 511 profiles in the paediatric groups were calculated based on the individual simulations of the population
 512 representatives according to the study age ranges and were compared to the mean clinical data. Mean
 513 simulated profiles were calculated for three different dosing scenarios: (i) fasted state conditions, (ii)
 514 fed state conditions using GTT scaling for all population representatives based on the homogenized
 515 reference meal, and (iii) age-dependent fed state conditions employing infant formula for population
 516 representatives < 2.5 h and homogenized reference meal for population representatives > 2.5 yr.

517 **Table III** Adjusted ibuprofen gastric transit time (GTT) values employing zero order emptying kinetics
 518 for beagles and paediatric population representatives based on meal caloric content.

Meal	Beagle dog		Infant		Infant/Child		Child			
	2-year-old, 10 kg body weight ^a		12-month-old, 9.5 kg body weight ^b		2-year-old, 12.9 kg body weight ^c		6-year-old, 23 kg body weight ^{b, c}		11 ^c -12 ^b year-old, 43.6/48.6 kg body weight ^d	
	Caloric content (kcal)	GTT (h)	Caloric content (kcal)	GTT (h)	Caloric content (kcal)	GTT (h)	Caloric content (kcal)	GTT (h)	Caloric content (kcal)	GTT (h)
Reference meal	200	1.1	170	0.94	200	1.1	260	1.43	340	1.87
Infant formula	100	1.1	170	1.87	200	2.2	-	-	-	-

519 ^a mean age and body weight of the male beagles (n=6)

520 ^b population representative (38)

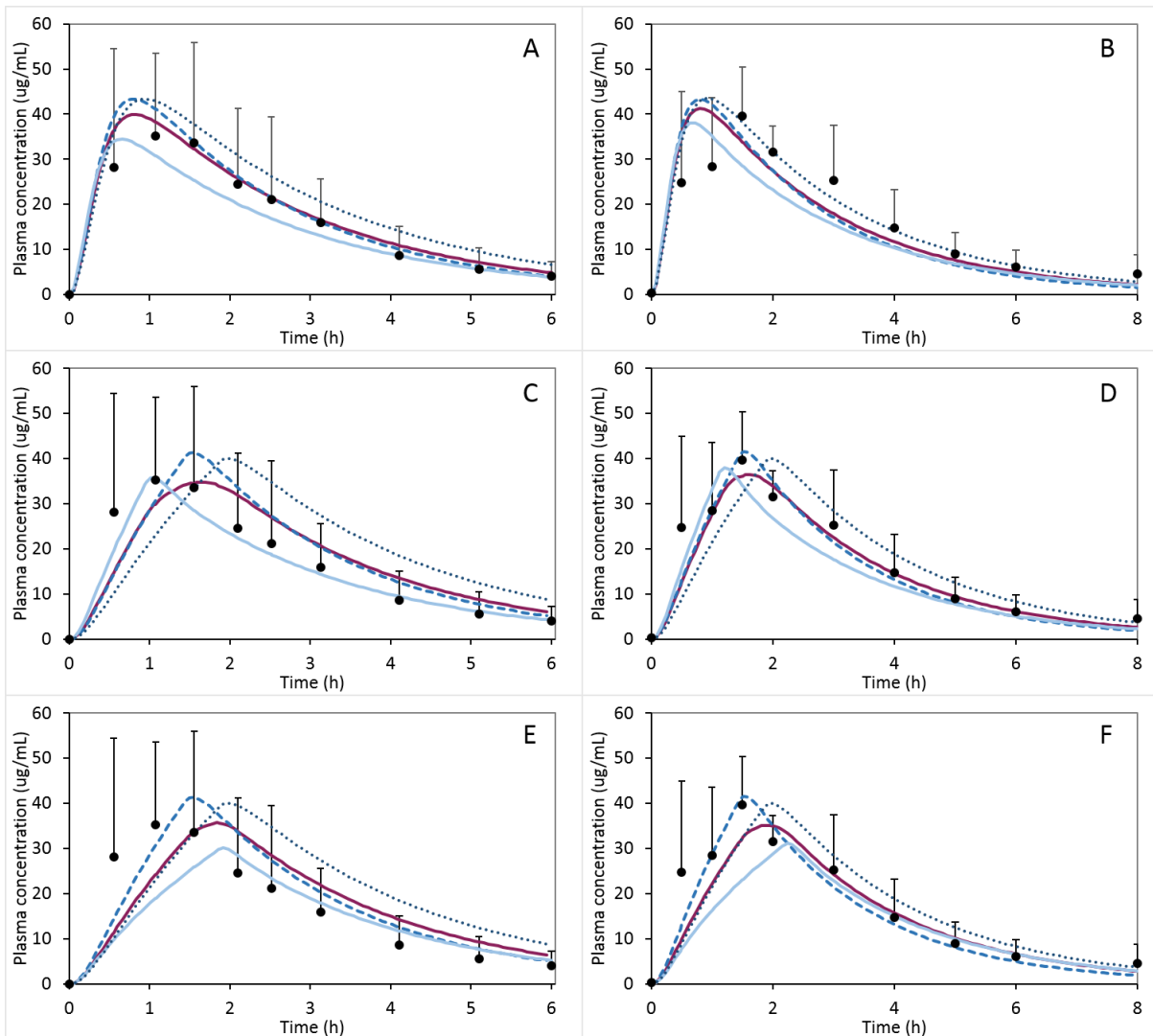
521 ^c population representative (37)

522 ^d the recommended average daily energy needs for the 11- and 12-year-old population
 523 representatives were the same, resulting in the same caloric content per meal and adjusted GTT value
 524 for these population representatives

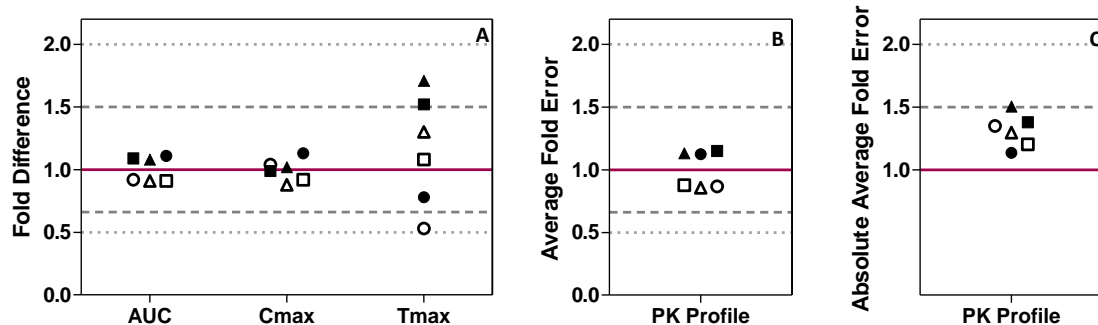
525

526 The resulting individual and mean simulated plasma concentration-time profiles based on the two
 527 study datasets are presented in Figure 6 and the respective model evaluation criteria are presented
 528 in Figure 7. Using the adjusted GTT from the canine absorption model (0.25 h) to simulate fasted state
 529 conditions in the target paediatric populations, reasonable simulations were achieved for the mean
 530 plasma concentration data for the mixed paediatric population Figure 6A, AAFE 1.135 (38). On the
 531 other hand, simulations for the children age group (37) appeared to overestimate mean observed
 532 plasma concentrations at early times and underestimate T_{max} (Figure 6B and Figure 7A), leading to an
 533 overall simulation inaccuracy (AAFE 1.350). Simulations using the ibuprofen reference-meal fed state
 534 performance in beagles and following zero order GE resulted in an overall ibuprofen absorption delay
 535 unlike *in vivo* mean observations in the mixed population, Figure 6C. For the children population, the
 536 application of adjusted reference-meal fed state conditions appeared to improve model estimations
 537 (Figure 6D, AAFE 1.203) compared to fasted state calculations (Figure 7A and C). Simulations with
 538 adjusted infant-formula fed state conditions based on ibuprofen performance in beagles for
 539 population representatives younger than 2.5 years in the paediatric population are shown in
 540 Figure 6E and F. Resulting mean simulations for the mixed population underestimated the observed
 541 mean early plasma levels and could not capture the overall ibuprofen performance *in vivo* with
 542 AAFE 1.504, (Figure 7A and C). Consideration of the infant formula-fed state conditions for the children
 543 dataset (37), as for mixed populations, resulted in delayed estimated absorption (Figure 6F), unlike
 544 observation from the mean profile in the clinical dataset, thereby leading to some simulation
 545 inaccuracies (Figure 7A and C). Lastly, despite the trends observed for the simulations vs. the mean

546 observed profiles, it is important to note that simulations for all three dosing conditions fell within the
 547 observed variability of the study in the majority of cases (Figure 6).
 548



549 **Figure 6** Simulated ibuprofen plasma concentration-time profiles (lines) following oral administration of
 550 ibuprofen under different dosing conditions based on drug formulation performance in beagles. Thin light
 551 blue continuous line (–) 1-year-old population representative (A, C, E) or 2-year-old child (B, D, F), dashed
 552 blue line (– –) 6-year-old child, dotted line (···) 12-year-old child (A, C, E) or 11-year-old child (B, D, F), bold purple
 553 continuous lines (–) mean profiles for the three age groups. Fasted state conditions (A, B); reference-meal
 554 fed state conditions (> 2.5 years) and infant-formula fed state conditions (< 2.5 years) (E, F). Symbols and error bars denote mean observed plasma levels and standard
 555 deviations (Brown *et al.*, 1992 (38); A, C, E) and (Walson *et al.*, 1989 (37); B, D, F).
 556
 557



558
 559 **Figure 7** Fold Difference (simulated/observed) for AUC_{0-8h}, C_{max}, and T_{max} (A), Average Fold Error (B), and
 560 Absolute Average Fold Error (C) for the mean profile from the mixed population group (closed symbols,
 561 Brown *et al.* 1992 (38)) and children population (open symbols, Walson *et al.* 1989 (37)) under fasted state
 562 conditions (circles), reference-meal fed state conditions (> 2.5 years) and infant-formula fed state conditions
 563 (< 2.5 years) and infant-formula fed state conditions (< 2.5 years) (triangles). The solid line represents the
 564 line of unity, grey dashed lines 0.66-1.5 range indicating successful simulations, and grey dotted lines the
 565 0.5-2 range indicating adequate simulations.

566

567 [Parameter sensitivity analysis](#)

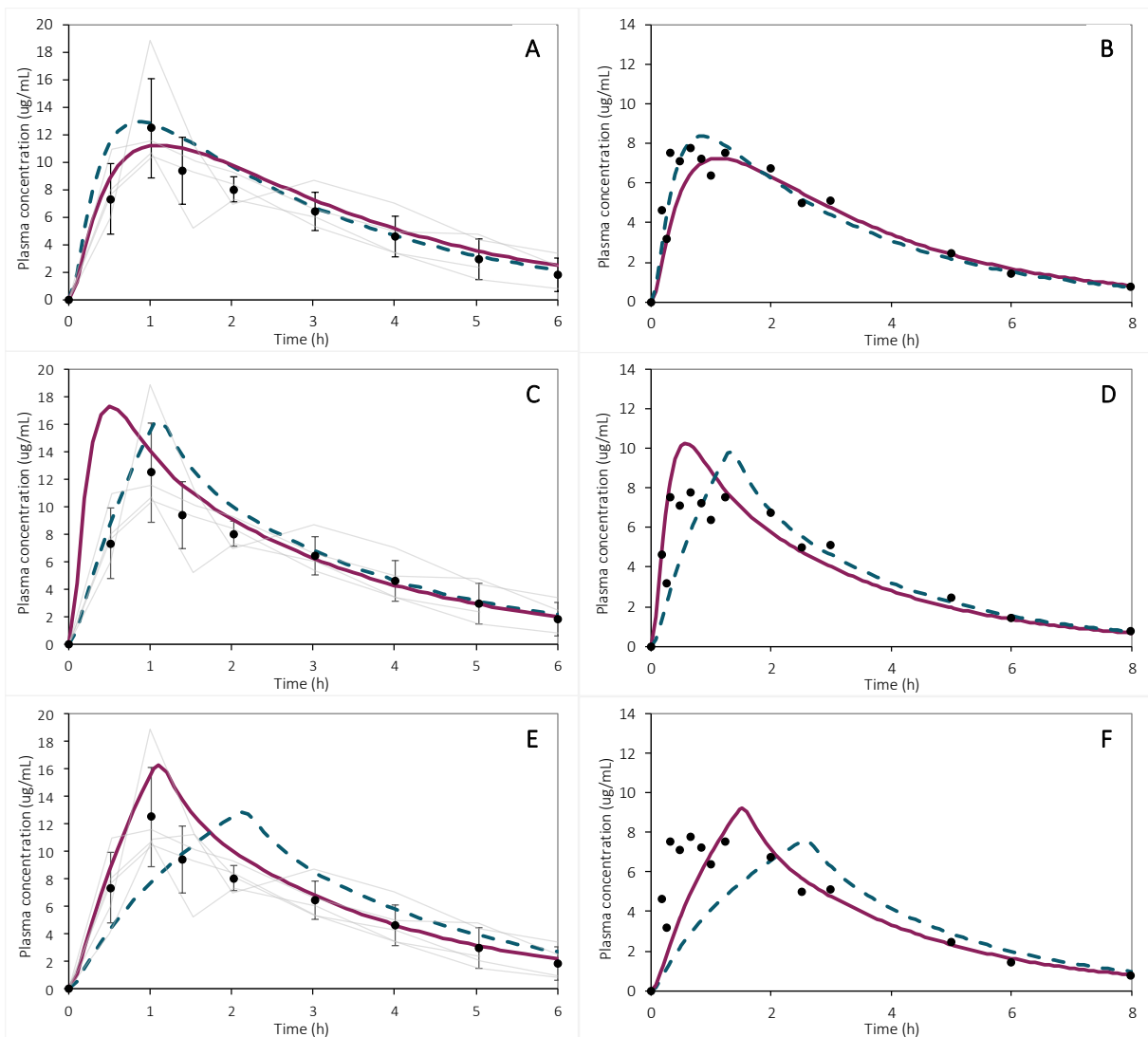
568 Parameters related to drug/drug formulation properties, physiology, and dosing conditions were
 569 investigated for the ibuprofen dog PBPK model (Table B-SVI). Greatest impact on drug absorption was
 570 observed regarding gastric transit times prolongation resulting in lower peak exposure and longer
 571 times to reach C_{max}, Figure B-S9 and Figure B-S11. Increase in liver first pass metabolism resulted in
 572 lower plasma levels and total exposure and peak exposure (Figure B-S10 and Figure B-S12). As for
 573 paracetamol, only after 10-fold permeability decrease ibuprofen drug absorption was retarded.
 574 Additionally, pH lowering in the duodenum resulted in slightly prolonged T_{max} and lowered C_{max} values,
 575 while gastric and jejunal pH had little to no impact on ibuprofen performance in beagles.

576

577 [Comparison of the usefulness of canine and human adult bioavailability data of](#) 578 [paracetamol and ibuprofen for exposure extrapolation to paediatrics](#)

579 Using GastroPlus V9.7, the beagle based PBPK model led to successful simulations of paracetamol
 580 performance in infants under fasted state conditions; likewise, extrapolation of fasted state data in
 581 human adults resulted in successful simulations of paracetamol performance in infants
 582 (Figure 8A and B). It might be worth noting that under fasted state conditions, a slightly greater
 583 absorption delay was estimated based on human adult data (Figure 8A and B). Simulations based on
 584 human adult data suggested that infant-formula fed state conditions were suitable to simulate mean
 585 paracetamol exposure in infants, while the same dosing conditions applied in beagles led to less

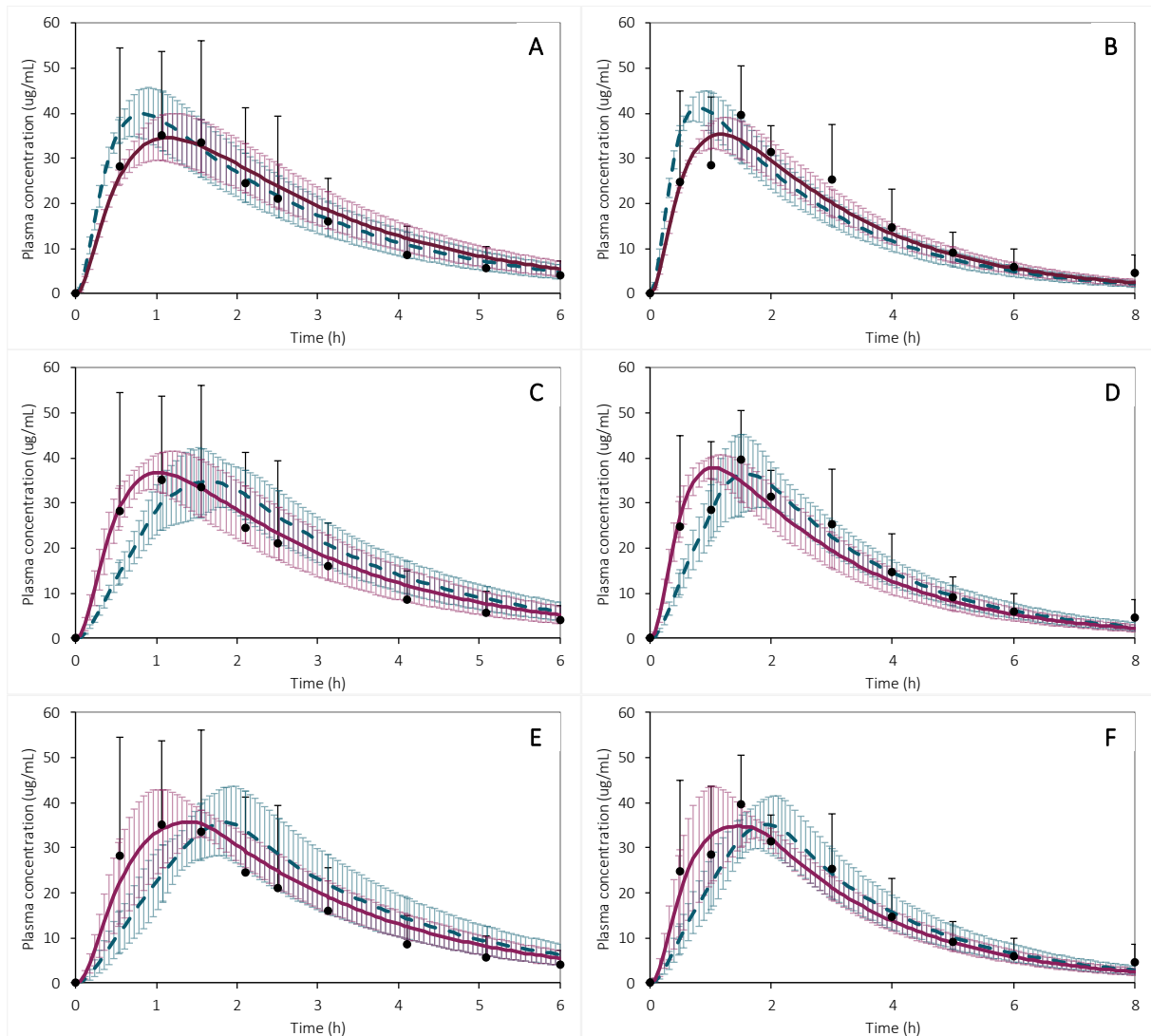
586 adequate simulations, (Figure 8E and F and Figure B-S13). Exposure extrapolation based on reference-
 587 meal fed state conditions (solid-liquid) in adults was less useful for capturing performance in infants
 588 based on the mean observed profiles, as indicated by the difference in simulated vs observed T_{max} . In
 589 contrast, when extrapolations were based on the beagle model, the reference-meal fed state
 590 conditions appeared to be closer to the average PK profiles and the observed T_{max} (Figure 8C and D
 591 and Figure B-S13). Furthermore, GE order appeared different in the canine and human adult
 592 simulations of the reference-meal fed state conditions, zero vs. first order GE process, respectively
 593 (Figure 8C and D).



594
 595 **Figure 8** Comparison of simulated plasma paracetamol levels in a population representative using PBPK
 596 models based on human adult bioavailability data (purple continuous lines, (24)) vs. Beagle bioavailability
 597 data (blue dashed lines, present study) under (A, B) fasted state conditions, (C, D) reference-meal fed state
 598 conditions, and (E, F) infant-formula fed state conditions. Left panel (Hopkins et al. 1990 (36); A, C, E) with
 599 a population representative of 4 months (study age range 2-6 months), individual observed plasma
 600 concentration-time profiles depicted as grey lines, observed mean concentrations and standard deviations
 601 depicted with black symbols and error bars; right panel (Walson et al., 2013 (35); B, D, E) with a population

602 representative of 10 months (study age range 3-36 months), observed mean concentrations depicted with
603 black symbols.

604 Ibuprofen simulations based on product performance under fasted state conditions in adults led to
605 successful simulations for the paediatric studies (37,38); adequate simulations were achieved using
606 the beagle-based model under fasted state conditions (Figure 9A and B and Figure B-S14). As for
607 paracetamol, simulated ibuprofen GE (MGTT) under fasted state conditions appeared somewhat
608 faster in canine data as opposed to human adults (Figure 9A and B).



609 **Figure 9** Comparison of mean simulated plasma ibuprofen levels in mixed paediatric populations using
610 PBPK models based on human adult bioavailability data (purple continuous lines and error bars, (25)) vs.
611 beagle bioavailability data (blue dashed lines and blue error bars, present study) under (A, B) fasted state
612 conditions, (C, D) reference-meal fed state conditions, and (E, F) reference-meal fed state conditions for
613 children and infant formula-fed state conditions for subjects < 2.5 years. Left panel (Brown et al., 1992 (38);
614 A, C, E) with study age range 0.3-12 years and right panel (Walson et al., 1989 (37); B, D, F) with study age
615 range 2-12 years, observed mean concentrations and standard deviations depicted with black symbols and
616 error bars.
617

618 Extrapolations based on the human adult model under reference-meal fed state conditions (solid-
619 liquid) and infant-formula fed state conditions successfully matched data observed in paediatric
620 groups (Figure 9C-F and Figure B-S14). In contrast, exposure simulations of the canine model based
621 on the reference-meal fed state conditions, but not infant-formula fed state conditions, were able to
622 capture the mean *in vivo* performance observed in paediatric patients (Figure 9C-F and Figure B-S14).
623 As for paracetamol, under the reference-meal fed state conditions, differences in ibuprofen GE
624 kinetics could be observed in human adults versus canine data, i.e., first versus zero order apparent
625 GE processes. Overall, as the simulations under different dosing conditions appeared to be matching
626 observed *in vivo* concentrations and to be within the study variability, therefore, comparisons
627 regarding the usefulness of human vs. dog as basis for oral model translation to paediatric populations
628 should be interpreted as indication of a trend, rather than generalizing finding.

629

630 Discussion

631 In the present study we collected paracetamol and ibuprofen plasma data in beagles, after
632 administering paediatric formulations under various dosing conditions, in order to evaluate their
633 usefulness in informing the plasma profile in simulations of systemic exposure in paediatric
634 populations. Simulations outcomes were then compared to the outcomes of simulations based on
635 published plasma data collected after administering the same formulations under various dosing
636 conditions to human adults.

637 .

638 Within the preclinical investigation under fasted state conditions, paracetamol and ibuprofen
639 exhibited rapid absorption (Figure 2 and Figure 5). In the paracetamol canine PBPK model, the
640 adjusted GTT value fell within physiologically observed GE half-life and Tmax reports (47–50). In this
641 context, it should be noted that the adjusted GTT value represents the formulation's gastric transit
642 time, rather than a general GE time for a clear fluid. Under fasted conditions, the application of HCl/KCl
643 pretreatment appeared not to affect paracetamol performance or GE substantially in the present
644 study; no effects were expected based on paracetamol high solubility and the drugs ionization
645 properties. Although ibuprofen is a weak acid and elevated pH levels in the fasted canine stomach
646 (33,34) could potentially impact drug performance, no considerable changes were observed with
647 respect to the ACAT™ physiology parameters employed to adequately describe drug behavior *in vivo*.
648 In the present investigation, the utilization of the HCl/KCl pre-treatment indicated no noticeable
649 impact on the two highly permeable drugs. Impact of acidifying pretreatment is expected to be more

650 pronounced for weakly basic lipophilic compounds, which rely on dissolution in the acidic stomach
651 environment to allow for supersaturation and absorption upon gastro-intestinal transfer or for
652 modified-release formulations utilizing functional pH-sensitive polymers (18,33,51).

653

654 Interestingly, in the present study, despite the two-fold difference in caloric content between the
655 homogenized reference meal (200 kcal) and the infant formula (100 kcal), the two meals resulted in
656 similar paracetamol/ibuprofen absorption delay and could be described by the same GE rate order
657 and GTT for the two meals. Gastric emptying of drug product and chyme under post-prandial
658 conditions is a complex process that is governed by multiple factors such as meal energy content,
659 volume, solid vs. liquid texture, viscosity, density, particle size of gastric contents, and osmolarity, to
660 name some (e.g., 52). Multiple investigations have showcased that increase of meal amounts and
661 calorific content results in a delay of gastric emptying in comparison to meals with fewer calories in
662 dogs (53–56). In comparison to humans where osmoreceptors providing the feedback leading to
663 gastric emptying delay are located in the duodenum, in dogs these receptors were found in the
664 jejunum and not in the first duodenal part (57,58). In the present beagle study, additional factors
665 might contribute to the overall GE of the two meals, such factors could be meal viscosity or volume
666 (59–63) , while osmolarity appeared to play a minor role in comparison to the presence of nutrients.
667 It should be noted that volume effects on GE were more evident at volumes higher than the ones
668 utilized in the present study, i.e., 150-1200 mL (63).

669 In humans, caloric dependence of gastric emptying rate has been demonstrated in several
670 investigations (64–71), with differences in volumes appearing to be a minor contributor (72).
671 Additionally, interplay between volume and calorific density has been proposed to describe the fed
672 state GE half-life in adults, for volumes > 100 mL (73). In addition to the linear relationship assumed
673 in the present study to enable caloric-based translation, other scaling approaches for estimating meal-
674 dependent GE have been reported for adults (74), advanced *in vitro* models (52), meal types (75), and
675 breastfeeding in newborns/infants (76); the predictive capabilities of these approaches for different
676 meal types and populations are yet to be confirmed with further clinical evidence. Meal compositions,
677 calories, textures, and volumes evolve with age progression of the specific paediatric populations, e.g.,
678 liquid milk-based feeds for infants, semi-solid meals for infants and toddlers, solid small meals for pre-
679 school children and school children, and increased adult-like portions for adolescents (1); based on
680 this, greatest potential differences between paediatric populations and adults would be expected for
681 the youngest – newborns and infants. Although caloric regulation of GE has been established in adults,
682 the postprandial GE behavior and main contributors in paediatric subjects are less studied. An
683 investigation in 10 premature infants who received different amounts of calories at the same formula

684 volume (22 mL/kg BW) revealed that significant inhibition of GE was related to increasing caloric
685 density over the entire test duration, leading to the conclusion that GE regulation by caloric density in
686 premature infants was qualitatively similar to that in adults (77). Furthermore, in pre-term newborns,
687 duodenal activity following feeding increased for newborns receiving infant formula infusion, while
688 duodenal activity for diluted infant formula resembled duodenal activity following water (78).

689 It should be considered that although the reference meal utilized in the beagle study was
690 homogenized, while the reference meal in the clinical study was a solid-liquid meal chewed by the
691 volunteers (5), the different texture might not have been a key contributor. In a recent study
692 conducted in human healthy adults, the reference meal was homogenized to facilitate meal
693 administration via nasogastric tube and no pronounced differences were reported due to meal
694 homogenization in comparison to a chewed meal (79).

695 Based on the present *in vivo-in silico* investigation of paracetamol suspension performance in beagles
696 and subsequent translation to infants, fasted state dosing conditions in beagles appeared useful to
697 inform modeling for infant formulations. Beagle data collected after the homogenized reference meal
698 were also useful for simulating the mean plasma concentrations of the younger population
699 (2-6 months (36)), but not for simulating the mean plasma concentrations of the older population
700 (3-36 months (35)). In contrast, beagle data collected under infant-formula fed state conditions were
701 less useful for extrapolating to infants, indicated by the mismatch between the simulated and
702 observed T_{max} . For ibuprofen, fasted state performance in beagles appeared useful for simulating
703 clinical datasets in a mixed paediatric population (38), while adjusted fed state conditions using the
704 homogenized reference meal appeared to lead to adequately describe mean concentrations in the
705 children dataset (37). For both drugs, fasted state and reference-meal fed state bioavailability data in
706 beagles led to adequate representation of the mean observed PK profiles in the target paediatric
707 populations in most cases; while infant-formula fed state conditions overestimated the oral
708 absorption delay observed *in vivo* in paediatrics, in line with the misalignment of the simulated vs
709 observed T_{max} for this dosing condition. In contrast, extrapolation based on fasted state and infant-
710 formula fed bioavailability data in human adults appeared to capture well the mean observed data in
711 most paediatric/infant datasets. Despite these trends for the human-based and dog-based
712 extrapolation processes, the conclusions should be interpreted with caution, as the adequacy of the
713 simulations was based on a small number of paediatric patients. Furthermore, as the datasets were
714 collected from patient populations, the impact of the disease on drug intraluminal performance
715 cannot be excluded. The presented extrapolation methodology and different dosing conditions
716 deserve further, more comprehensive evaluation utilizing compounds with various biopharmaceutics

717 properties and formulation principles to allow for a clear conclusion on their usefulness within drug
718 product design and development.

719 For both model drugs, performed PSA for the beagle model indicated limited sensitivity to changes in
720 drug and/or physiology-related parameters, including the uncertainty pertaining to utilizing the in-
721 built 3-fold higher permeability for dogs vs. humans. Compared to humans, passive permeability in
722 dogs has been demonstrated to be higher, especially for drugs/compounds which are predominantly
723 absorbed via the paracellular route (17,80–82); the high permeability utilized in the canine models for
724 paracetamol and ibuprofen led to lack of preclinical model sensitivity regarding this parameter.
725 Conversely, the transcellular absorption pathway is expected to be similar for humans and dogs, which
726 is in line with the reported similar effective permeability in both species for two highly permeable
727 drugs (81). In addition to the passive permeability routes, anatomical differences between dogs and
728 humans can have an impact on the regional effective permeability of the drug (17). Employing human-
729 like Peff in the paracetamol and ibuprofen canine models had no impact on the canine simulations
730 and the estimated GE parameters under the applied dosing conditions; this indicated lack of
731 confounding effect of the employed Peff in the preclinical model for the estimated GE parameters for
732 the different dosing conditions. A further uncertainty pertaining to the regional
733 absorption/permeability in the virtual canine physiology could be the utilization of the Opt LogD SA/V
734 6.1 model to estimate ASF. The method selection for scaling of regional permeability in the virtual
735 ACAT™ physiologies should be decided with caution for the specific model drugs and adjusted if
736 further scientific evidence is available for specific cases (22,82). In the paediatric models (24,25),
737 sensitivity towards reduced permeability model was demonstrated for lower permeability resulting in
738 delayed absorption under fasted state conditions. The potentially higher permeability in dogs (and
739 lack of model sensitivity to permeability changes) could pose a challenge for translating or identifying
740 the rate-limiting absorption process in the preclinical species vs. humans. Careful consideration of
741 compound permeability and its adequate representation *in silico* is imperative in extrapolations to
742 paediatric populations; specifically in cases where permeability is a confirmed critical bioavailability
743 attribute, as intestinal barrier maturation occurs in infant age groups and permeability has been
744 identified as a parameter of uncertainty for paediatric extrapolations into young age groups (1,24,25).

745 Although beagles have been and still are used in preclinical formulation investigations for adults, their
746 usefulness for evaluation of product performance in paediatric patients has not been explored. Based
747 on the similarities of the human adult and canine GI tract, the beagle food effect model has proven its
748 utility in several cases in literature for predicting food effects in human adults (23,32,83,84). On the
749 other hand, studies have shown that food effects on total exposure and C_{max} in human adults were
750 not accurately captured by investigations performed in dogs (83,85). For celecoxib the increase in drug

751 exposure was 3-5-fold following food, while human adult food effect studies indicated only 11 %
752 increase in the fed state (85). In this context, within the present investigation, limited exposure effects
753 were expected for the two model drugs, however, differences were observed between human and
754 beagle regarding the observed absorption characteristics that could be linked to mechanical/physical
755 interaction of drug with the chyme, i.e., mixing and sieving events leading to different gastric transit
756 times. As paracetamol and ibuprofen are highly soluble and permeable in the upper SI, the observed
757 changes in drug performance among the different dosing conditions would be expected to be less
758 sensitive to differences in intraluminal fluid composition under the applied dosing conditions; gastric
759 transit time alterations as a function of prandial state can be a potential factor to explain the observed
760 *in vivo* performance. Differences in drug transit behavior was reflected in the simulations and affected
761 simulations adequacy for the paediatric populations studied, even for a simple drug product such as
762 an aqueous suspension. Implications for more complex formulations (e.g., enabling formulations) and
763 poorly water-soluble compounds with more challenging physicochemical properties deserve further
764 evaluation, building upon the understanding gained from the present investigation.

765 Concluding remarks

766

767 Despite the differences observed between the beagle-based and human adult-based model
768 predictions, the beagle appears suitable for investigating paediatric products of the two studied highly
769 soluble, highly permeable drugs in the upper small intestine at early drug product development stages,
770 when applying fasted and/or reference-meal fed state conditions for paracetamol and ibuprofen.
771 During later stages, human-based simulations for the two model drugs appeared superior in most of
772 the cases, especially regarding the usefulness of infant-formula fed state conditions. It should be noted
773 that the majority of simulations performed were within the error of the observed clinical data in the
774 paediatric studies and were within the targeted accuracy. A deeper understanding of the differences
775 regarding meal calorie- and texture-dependent drug GE between human adults and beagles could
776 improve pre-clinical protocols applied at present to investigate food effects. To overcome some of the
777 interspecies difference, the present work demonstrated an approach utilizing PBPK modeling for
778 paediatric formulation evaluation at an early development stage for two highly soluble and highly
779 permeable in the upper small intestine model drugs. Nevertheless, verification of the proposed
780 methodologies for infant formulation evaluation with broader spectrum of compounds with different
781 physicochemical properties as well as different formulation principles is required. Lastly, availability
782 of high-quality clinical data in infants is of paramount importance for evaluating the biopharmaceutics
783 tools and methodologies and confirmation of their reliability.

784

785 Acknowledgements

786 The authors are indebted to Sarah De Landtsheer and Gert Martens for the skillful handling of the
787 beagle study and to Herman Borghys and Koen Wuyts for their invaluable input during the beagle
788 study planning. The authors would like to thank SimulationsPlus Inc. for providing access to
789 GastroPlus™ 9.7.

790

791 [Declarations of interest: none.](#)

792 Funding

793 This work was supported by the Horizon 2020 Marie Skłodowska-Curie Innovative Training Networks
794 programme under grant agreement No. 674909.

795

References

1. Guimarães M, Stelova M, Holm R, Reppas C, Symillides M, Vertzoni M, et al. Biopharmaceutical considerations in paediatrics with a view to the evaluation of orally administered drug products - a PEARRL review. *J Pharm Pharmacol*. 2019;71(4):603–42.
2. Batchelor H. Influence of food on paediatric gastrointestinal drug absorption following oral administration: a review. *Children*. 2015;2(2):244–71.
3. Elder DP, Holm R, Kuentz M. Medicines for Pediatric Patients—Biopharmaceutical, Developmental, and Regulatory Considerations. *J Pharm Sci*. 2017;106(4):950–60.
4. CDER, Center for Drug Evaluation and Research Food F and DA. Assessing the Effects of Food on Drugs in INDs and NDAs - Clinical pharmacology considerations Guidance for industry. FDA Guid. 2022;(June). Available from: <https://www.fda.gov/media/121313/download>
5. Stelova M, Goumas K, Fotaki N, Holm R, Symillides M, Reppas C, et al. On the Design of Food Effect Studies in Adults for Extrapolating Oral Drug Absorption Data to Infants : an Exploratory Study Highlighting the Importance of Infant Food. *AAPS J*. 2020;22(6):1–11.
6. Wollmer E, Ungell A-L, Nicolas J-M, Klein S. Review of paediatric gastrointestinal physiology relevant to the absorption of orally administered medicines. *Adv Drug Deliv Rev*. 2022;181:114084.
7. Batchelor H, Kaukonen AM, Klein S, Davit B, Ju R, Ternik R, et al. Food effects in paediatric medicines development for products co-administered with food. *Int J Pharm*. 2018 Feb;536(2):530–5.
8. U.S. Department of Health and Human Services Food and Drug Administration. Leveraging Existing Clinical Data for Extrapolation to Pediatric Uses of Medical Devices. 2016 p. 1–37.
9. Pentafragka C, Symillides M, McAllister M, Dressman J, Vertzoni M, Reppas C. The impact of food intake on the luminal environment and performance of oral drug products with a view to *in vitro* and *in silico* simulations: a PEARRL review. *J Pharm Pharmacol*. 2018 Sep;
10. Van den Bergh A, Van Hemelryck S, Bevernage J, Van Peer A, Brewster M, Mackie C, et al. Preclinical Bioavailability Strategy for Decisions on Clinical Drug Formulation Development: An In Depth Analysis. *Mol Pharm*. 2018 Jul;15(7):2633–45.
11. Selen A, Dickinson PA, Müllertz A, Crison JR, Mistry HB, Cruañes MT, et al. The Biopharmaceutics Risk Assessment Roadmap for Optimizing Clinical Drug Product Performance. *J Pharm Sci*. 2014;103(11):3377–97.
12. Tistaert C, Heimbach T, Xia B, Parrott N, Samant TS, Kesisoglou F. Food Effect Projections via Physiologically Based Pharmacokinetic Modeling: Predictive Case Studies. *J Pharm Sci*. 2019 Jan 1;108(1):592–602.
13. Pepin XJH, Huckle JE, Alluri R V, Basu S, Dodd S, Parrott N, et al. Understanding Mechanisms of Food Effect and Developing Reliable PBPK Models Using a Middle-out Approach. *AAPS J*. 2021;23(1):12.
14. Koziolk M, Grimm M, Bollmann T, Schäfer KJ, Blattner SM, Lotz R, et al. Characterization of the GI transit conditions in Beagle dogs with a telemetric motility capsule. *Eur J Pharm Biopharm*. 2019;136(August 2018):221–30.

15. Sjögren E, Abrahamsson B, Augustijns P, Becker D, Bolger MB, Brewster M, et al. In vivo methods for drug absorption - Comparative physiologies, model selection, correlations with in vitro methods (IVIVC), and applications for formulation/API/excipient characterization including food effects. Vol. 57, *European Journal of Pharmaceutical Sciences*. 2014. 99–151 p.
16. Martinez MN, Papich MG. Factors influencing the gastric residence of dosage forms in dogs. *J Pharm Sci*. 2009;98(3):844–60.
17. Martinez MN, Mochel JP, Neuhoff S, Pade D. Comparison of Canine and Human Physiological Factors: Understanding Interspecies Differences that Impact Drug Pharmacokinetics. *AAPS J*. 2021;23(3).
18. Polentarutti B, Albery T, Dressman J, Abrahamsson B. Modification of gastric pH in the fasted dog. *J Pharm Pharmacol*. 2010;62(4):462–9.
19. Sagawa K, Li F, Liese R, Sutton SC. Fed and fasted gastric pH and gastric residence time in conscious beagle dogs. *J Pharm Sci*. 2009;98(7):2494–500.
20. Heikkinen AT, Fowler S, Gray L, Li J, Peng Y, Yadava P, et al. In vitro to in vivo extrapolation and physiologically based modeling of cytochrome P450 mediated metabolism in beagle dog gut wall and liver. *Mol Pharm*. 2013;10(4):1388–99.
21. Lin Z, Li M, Gehring R, Riviere JE. Development and application of a multiroute physiologically based pharmacokinetic model for oxytetracycline in dogs and humans. *J Pharm Sci*. 2015;104(1):233–43.
22. Kesisoglou F, Balakrishnan A, Manser K. Utility of PBPK Absorption Modeling to Guide Modified Release Formulation Development of Gaboxadol, a Highly Soluble Compound With Region-Dependent Absorption. *J Pharm Sci*. 2016;105(2):722–8.
23. Li X, Yang Y, Zhang Y, Wu C, Jiang Q, Wang W, et al. Justification of Biowaiver and Dissolution Rate Specifications for Piroxicam Immediate Release Products Based on Physiologically Based Pharmacokinetic Modeling: An In-Depth Analysis. *Mol Pharm*. 2019;16(9):3780–90.
24. Statelova M, Holm R, Fotaki N, Reppas C, Vertzoni M. Successful extrapolation of paracetamol exposure from adults to infants after oral administration of a paediatric aqueous suspension is highly dependent on the study dosing conditions. *AAPS J*. 2020;22(126):1–17.
25. Statelova M, Holm R, Fotaki N, Reppas C, Vertzoni M. Factors affecting successful extrapolation of ibuprofen exposure from adults to paediatric populations after oral administration of a paediatric aqueous suspension. *AAPS J*. 2020;In press.
26. Potthast H, Dressman JB, Junginger HE, Midha KK, Oeser H, Shah VP, et al. Biowaiver monographs for immediate release solid oral dosage forms: Ibuprofen. *J Pharm Sci*. 2005;94(10):2121–31.
27. Wu CY, Benet LZ. Predicting drug disposition via application of BCS: Transport/absorption/elimination interplay and development of a biopharmaceutics drug disposition classification system. *Pharm Res*. 2005;22(1):11–23.
28. European Medicines Agency E. Ibuprofen oral use immediate release formulations 200 - 800 mg product-specific bioequivalence guidance. 2018. p. 1–4.
29. Atkinson HC, Stanescu I, Frampton C, Salem II, Beasley CPH, Robson R. Pharmacokinetics and bioavailability of a fixed-dose combination of ibuprofen and paracetamol after intravenous and oral administration. *Clin Drug Investig*. 2015;35(10):625–32.
30. Wright CE, Antal EJ, Gillespie WR, Albert KS. Ibuprofen and acetaminophen kinetics when

- taken concurrently. *Clin Pharmacol Ther.* 1983;34(5):707–10.
31. European Medicines Agency (EMA). Guideline on the investigation of drug interactions. Guid Doc [Internet]. 2012;44(June):1–59. Available from: https://www.ema.europa.eu/en/documents/scientific-guideline/guideline-investigation-drug-interactions-revision-1_en.pdf
 32. Wu Y, Loper A, Landis E, Hettrick L, Novak L, Lynn K, et al. The role of biopharmaceutics in the development of a clinical nanoparticle formulation of MK-0869: A Beagle dog model predicts improved bioavailability and diminished food effect on absorption in human. *Int J Pharm.* 2004;285(1–2):135–46.
 33. Zane P, Guo Z, Macgerorge D, Vicat P, Ollier C. Use of the pentagastrin dog model to explore the food effects on formulations in early drug development. *Eur J Pharm Sci.* 2014;57(1):207–13.
 34. Akimoto M, Nagahata N, Furuya a, Fukushima K, Higuchi S, Suwa T. Gastric pH profiles of beagle dogs and their use as an alternative to human testing. *Eur J Pharm Biopharm.* 2000;49(2):99–102.
 35. Walson PD, Halvorsen M, Edge J, Casavant MJ, Kelley MT. Pharmacokinetic Comparison of Acetaminophen Elixir Versus Suppositories in Vaccinated Infants (Aged 3 to 36 Months): A Single-Dose, Open-Label, Randomized, Parallel-Group Design. *Clin Ther.* 2013;35(2):135–40.
 36. Hopkins CS, Underhill S, Booker PD. Pharmacokinetics of paracetamol after cardiac surgery. *Arch Dis Child.* 1990;65(9):971–6.
 37. Walson PD, Galletta G, Pharm D, Braden NT, Alexander L, Columbus BS. Ibuprofen, acetaminophen, and placebo treatment of febrile children. *Clin Pharmacol Ther.* 1989;46(1):9–17.
 38. Brown RD, Wilson JT, Kearns GL, Eichler VF, Johnson VA, Bertrand KM. Single-dose pharmacokinetics of ibuprofen and acetaminophen in febrile children. *J Clin Pharmacol.* 1992;32:232–41.
 39. Gobeau N, Stringer R, De Buck S, Tuntland T, Faller B. Evaluation of the GastroPlus™ Advanced Compartmental and Transit (ACAT) Model in Early Discovery. *Pharm Res.* 2016;33(9):2126–39.
 40. Xia B, Heimbach T, Lin TH, Li S, Zhang H, Sheng J, et al. Utility of physiologically based modeling and preclinical in vitro/in vivo data to mitigate positive food effect in a BCS class 2 compound. *AAPS PharmSciTech.* 2013;14(3):1255–66.
 41. Mudie DM, Stewart AM, Rosales JA, Adam MS, Morgen MM, Vodak DT. In vitro-in silico tools for streamlined development of acalabrutinib amorphous solid dispersion tablets. *Pharmaceutics.* 2021;13(12).
 42. Parrott N, Lukacova V, Fraczkiewicz G, Bolger MB. Predicting pharmacokinetics of drugs using physiologically based modeling - Application to food effects. *AAPS J.* 2009;11(1):45–53.
 43. Obach RS, Baxter JG, Liston TE, Silber BM, Jones BC, Macintyre F, et al. The Prediction of Human Pharmacokinetic Parameters from Preclinical and In Vitro Metabolism Data. *J Pharmacol Exp Ther.* 1997 Oct;283(1):46 LP – 58.
 44. Mahmood I, Ahmad T, Mansoor N, Sharib SM. Prediction of Clearance in Neonates and Infants (≤ 3 Months of Age) for Drugs That Are Glucuronidated: A Comparative Study Between Allometric Scaling and Physiologically Based Pharmacokinetic Modeling. *J Clin*

- Pharmacol. 2017;57(4):476–83.
45. Zuppa A, Hammer G, Barrett J, Kenney B, Kassir N, Moukassi S, et al. Safety and Population Pharmacokinetic Analysis of Intravenous Acetaminophen in Neonates, Infants, Children, and Adolescents With Pain or Fever. *J Pediatr Pharmacol Ther.* 2011;16(4):246–61.
 46. Neirinckx E, Vervaeck C, De Boever S, Remon JP, Gommeren K, Daminet S, et al. Species comparison of oral bioavailability, first-pass metabolism and pharmacokinetics of acetaminophen. *Res Vet Sci.* 2010;89(1):113–9.
 47. Sjödin L, Visser S, Al-Saffar A. Using pharmacokinetic modeling to determine the effect of drug and food on gastrointestinal transit in dogs. *J Pharmacol Toxicol Methods.* 2011;64(1):42–52.
 48. Koyanagi T, Yamaura Y, Yano K, Kim S, Yamazaki H. Age-related pharmacokinetic changes of acetaminophen, antipyrine, diazepam, diphenhydramine, and ofloxacin in male cynomolgus monkeys and beagle dogs. *Xenobiotica.* 2014;44(10):893–901.
 49. Sagara K, Mizuta H, Ohshiko M, Shibata M, Haga K. Relationship Between the Phasic Period of Interdigestive Migrating Contraction and the Systemic Bioavailability of Acetaminophen in Dogs. Vol. 12, *Pharmaceutical Research: An Official Journal of the American Association of Pharmaceutical Scientists.* 1995. p. 594–8.
 50. Madsen M, Enomoto H, Messenger K, Papich MG. Effects of housing environment on oral absorption of acetaminophen in healthy Beagles. Vol. 83. 2022.
 51. Fancher RM, Zhang H, Slecicka B, Derbin G, Rockar R, Marathe P. Development of a canine model to enable the preclinical assessment of pH-dependent absorption of test compounds. *J Pharm Sci.* 2011 Jul;100(7):2979–88.
 52. Smeets-Peeters M, Watson T, Minekus M, Havenaar R. A review of the physiology of the canine digestive tract related to the development of in vitro systems. *Nutr Res Rev.* 1998 Jun;11(1):45–69.
 53. Mizuta H, Kawazoe Y, Haga K, Ogawa K. Effects of meals on gastric emptying and small intestinal transit times of a suspension in the beagle dog assessed using acetaminophen and salicylazosulfapyridine as markers. *Chem Pharm Bull.* 1990;38(8):2224–7.
 54. Tanaka T, Mizumoto A, Haga N, Itoh Z. A new method to measure gastric emptying in conscious dogs: A validity study and effects of EM523 and L-NNA. *Am J Physiol - Gastrointest Liver Physiol.* 1997;272(4 35-4).
 55. Wyse CA, Preston T, Love S, Morrison DJ, Cooper JM, Yam PS. Use of the ¹³C-octanoic acid breath test for assessment of solid-phase gastric emptying in dogs. *Am J Vet Res.* 2001;62(12):1939–44.
 56. Meyer JH, Elashoff JD, Domeck M, Levy A, Jehn D, Hlinka M, et al. Control of canine gastric emptying of fat by lipolytic products. *Am J Physiol - Gastrointest Liver Physiol.* 1994;266(6 29-6).
 57. Cooke AR, Clark ED. Effect of First Part of Duodenum on Gastric Emptying in Dogs: Response to Acid, Fat, Glucose, and Neural Blockade. *Gastroenterology [Internet].* 1976;70(4):550–5. Available from: [http://dx.doi.org/10.1016/S0016-5085\(76\)80494-5](http://dx.doi.org/10.1016/S0016-5085(76)80494-5)
 58. Cooke AR. Localization of Receptors Inhibiting Gastric Emptying in the Gut. *Gastroenterology.* 1977;72(5):875–80.
 59. Gupta PK, Robinson JR. Effect of volume and viscosity of coadministered fluid on

- gastrointestinal distribution of small particles. *Int J Pharm.* 1995;125(2):185–93.
60. Gupta PK, Robinson JR. Gastric emptying of liquids in the fasted dog. *Int J Pharm.* 1988;43(1–2):45–52.
 61. Ehrlein H -J, Pröve J. Effect of Viscosity of Test Meals on Gastric Emptying in Dogs. *Q J Exp Physiol.* 1982;67(3):419–25.
 62. Reppas C, Dressman JB. Viscosity modulates blood glucose response to nutrient solutions in dogs. *Diabetes Res Clin Pract.* 1992;17(2):81–8.
 63. Lin HC, Elashoff JD, Gu Y, Meyer JH. Effect of meal volume on gastric emptying. *Neurogastroenterol Motil.* 1992;4(3):157–63.
 64. Collins PJ, Horowitz M, Cook DJ, Harding PE, Shearman DJ. Gastric emptying in normal subjects - a reproducible technique using a single scintillation camera and computer system. *Gut.* 1983;24(12):1117–25.
 65. Kong F, Singh RP. Disintegration of solid foods in human stomach. *J Food Sci.* 2008;73(5).
 66. Shafer RB, Levine AS, Marlette JM, Morley JE. Do calories, osmolality, or calcium determine gastric emptying? *Am J Physiol - Regul Integr Comp Physiol.* 1985;17(4):479–83.
 67. Halawi H, Camilleri M, Acosta A, Vazquez-Roque M, Oduyebo I, Burton D, et al. Relationship of gastric emptying or accommodation with satiation, satiety, and postprandial symptoms in health. *Am J Physiol - Gastrointest Liver Physiol.* 2017;313(5):G442–7.
 68. Guiastrennec B, Sonne DP, Hansen M, Bagger JI, Lund A, Rehfeld JF, et al. Mechanism-Based Modeling of Gastric Emptying Rate and Gallbladder Emptying in Response to Caloric Intake. *CPT pharmacometrics Syst Pharmacol.* 2016 Dec;5(12):692–700.
 69. Calbet JAL, MacLean DA. Role of caloric content on gastric emptying in humans. *J Physiol.* 1997;498(2):553–9.
 70. Okabe T, Terashima H, Sakamoto A. A comparison of gastric emptying of soluble solid meals and clear fluids matched for volume and energy content: a pilot crossover study. *Anaesthesia.* 2017;72(11):1344–50.
 71. Okabe T, Terashima H, Sakamoto A. Determinants of liquid gastric emptying: comparisons between milk and isocalorically adjusted clear fluids. *Br J Anaesth.* 2015;114(1):77–82.
 72. Noakes TD, Rehrer NJ, Maughan RJ. The importance of volume in regulating gastric emptying. *Med Sci Sports Exerc.* 1991 Mar;23(3):307–13.
 73. Hunt JN, Stubbs DF. The volume and energy content of meals as determinants of gastric emptying. *J Physiol.* 1975;245(1):209–25.
 74. Winter F, Schick P, Weitschies W. Bridging the Gap between Food Effects under Clinical Trial Conditions and Real Life: Modeling Delayed Gastric Emptying of Drug Substances and Gastric Content Volume Based on Meal Characteristics. *Mol Pharm.* 2023 Feb 6;20(2):1039–49.
 75. Johnson TN, Bonner JJ, Tucker GT, Turner DB, Jamei M. Development and application of a physiologically-based model of paediatric oral drug absorption. *Eur J Pharm Sci.* 2018;
 76. Yeung CHT, Fong S, Malik PR V, Edginton AN. Quantifying breast milk intake by term and preterm infants for input into paediatric physiologically based pharmacokinetic models. *Matern Child Nutr.* 2020 Apr;16(2):e12938.
 77. Siegel M, Lebenthal E, Krantz B. Effect of caloric density on gastric emptying in premature

- infants. *J Pediatr*. 1984;104(1):118–22.
78. Baker JH, Berseth CL. Duodenal motor responses in preterm infants fed formula with varying concentrations and rates of infusion. *Pediatr Res*. 1997 Nov;42(5):618–22.
 79. Pentafragka C, Vertzoni M, Symillides M, Goumas K, Reppas C. Disposition of two highly permeable drugs in the upper gastrointestinal lumen of healthy adults after a standard high-calorie, high-fat meal. *Eur J Pharm Sci*. 2020;149(January).
 80. He YL, Murby S, Warhurst G, Gifford L, Walker D, Ayrton J, et al. Species differences in size discrimination in the paracellular pathway reflected by oral bioavailability of poly(ethylene glycol) and D-peptides. *J Pharm Sci*. 1998;87(5):626–33.
 81. Dahlgren D, Roos C, Johansson P, Lundqvist A, Tannergren C, Abrahamsson B, et al. Regional Intestinal Permeability in Dogs: Biopharmaceutical Aspects for Development of Oral Modified-Release Dosage Forms. *Mol Pharm*. 2016 Sep 6;13(9):3022–33.
 82. Eckernäs E, Tannergren C. Physiologically Based Biopharmaceutics Modeling of Regional and Colon Absorption in Dogs. *Mol Pharm*. 2021;18(4):1699–710.
 83. Lentz KA, Quitko M, Morgan DG, Jr. JEG, Gleason C, Marathe PH. Development and validation of a preclinical food effect model. *J Pharm Sci*. 2007;96(2):459–72.
 84. Cook CS, Hauswald CL, Grahn AY, Kowalski K, Karim A, Koch R, et al. Suitability of the dog as an animal model for evaluating theophylline absorption and food effects from different formulations. *Int J Pharm*. 1990;60(2):125–32.
 85. Paulson SK, Vaughn MB, Jessen SM, Lawal Y, Gresk CJ, Yan B, et al. Pharmacokinetics of celecoxib after oral administration in dogs and humans: effect of food and site of absorption. *J Pharmacol Exp Ther*. 2001;297(2):638–45.

1 Usefulness of the beagle model in the
2 evaluation of paracetamol and ibuprofen
3 exposure after oral administration to
4 paediatric populations: An exploratory
5 study

6 [Supplementary Information](#)

7

8 Marina Statelova^{1,2}, René Holm^{3,4}, Nikoletta Fotaki⁵, Christos Reppas¹, Maria Vertzoni^{1*}

9 ¹ Department of Pharmacy, National and Kapodistrian University of Athens, Athens, Greece

10 ² Present affiliation: ARD Dissolution & Biopharmaceutics, Novartis Pharma AG, Basel, Switzerland

11 ³ Drug Product Development, Janssen Research and Development, Johnson & Johnson, Beerse,

12 Belgium

13 ⁴ Department of Physics, Chemistry and Pharmacy, University of Southern Denmark, 5230 Odense,

14 Denmark

15 ⁵ Department of Pharmacy and Pharmacology, University of Bath, Bath, UK

16

17 * Correspondence to:

18 [Dr Maria Vertzoni](#)

19 Department of Pharmacy

20 National and Kapodistrian University of Athens,

21 Panepistimiopolis,

22 157 84 Zografou, Greece

23 Tel. +30 210 727 4035

24 E-mail: vertzoni@pharm.uoa.gr

25 Part A: Experimental (drug determination in plasma samples)

26 Paracetamol and ibuprofen were analyzed separately using a different sample preparation procedure
27 for each drug. Protein precipitation with subsequent centrifugation, and dilution were applied as
28 sample treatment procedure according to previously described methods (1–3). The diluted
29 supernatant was analysed via ultra-high-pressure liquid chromatography (UPLC) employing an Acquity
30 UPLC System (Waters Corporation, Milford, MA USA).

31

32 *Chromatographic conditions*

33 The Acquity UPLC system utilized in this study consisted of a binary solvent manager, sample manager
34 with integral column temperature control, coupled with a photodiode array (PDA) detector. System
35 control, data acquisition and processing were performed using the Empower 3[®] chromatography data
36 software (Waters Corporation, Milford, MA USA). Sample separation was achieved on an Acquity
37 UPLC™ BEH C₁₈ column (2.1 mm x 50 mm, 1.7 μm, 130Å) equipped with an ACQUITY UPLC™ BEH C₁₈
38 VanGuard pre-column (2.1 mm X 5 mm, 130Å, 1.7 μm). Gradient elution was performed using 0.1 %
39 trifluoroacetic acid in water (v/v) as Solvent A and ACN as Solvent B, shown in Table A-S1 Optimal
40 separation was achieved with a constant column temperature of 55° C at a flow rate of 0.4 mL/min
41 for paracetamol and 0.6 mL/min for ibuprofen.

42 **Table A-SI** Gradient elution steps applied in the UPLC method

Elution	Solvent A	Solvent B	Time (min)
Isocratic	90	10	0-0.8
Linear gradient	0	100	0.8-2.8
Isocratic	0	100	2.8-3.1
Linear gradient	90	10	3.1-3.2
Isocratic	90	10	3.2-4.0

43

44 *Paracetamol analysis*

45 The paracetamol bioassay involved precipitation of 100 μL plasma sample with 200 μL 10% aqueous
46 dilution of TFA (v/v), followed by vortex-mixing over one minute and centrifugation over 10 minutes
47 at 10° C and 12 000 g (Centrifuge 5430 R, Eppendorf AG, Germany). After the collection of 150 μL clear
48 supernatant and dilution with 150 μL water, 8 μL were injected into the UPLC system. The detection
49 wavelength was 242 nm. Calibration curves were linear between the ranges 0.01 – 6 μg/mL, R₂
50 > 0.9991 with a lower limit of quantification of 60 ng/mL in plasma. Quantification of the samples

51 analyzed was performed using standards diluted in a 90:10 Solvent A:Solvent B mixture; each standard
52 was injected 3 times, and quality control standards were injected after every 10th injection performed
53 (percent error <9.8%).

54 *Ibuprofen analysis*

55 The ibuprofen bioassay involved precipitation of 100 µL plasma sample acidified with 10 µL 5%
56 aqueous dilution of TFA (v/v) by addition of 190 µL ice-cold ACN, followed by vortex-mixing over one
57 minute and centrifugation over 10 minutes at 10° C and 12 000 g. After the collection of 150 µL clear
58 supernatant and dilution with 150 µL diluent mixture of 60:40 Solvent B:Solvent A (v/v), 8 µL were
59 injected into the UPLC system. Ibuprofen was detected at a wavelength of 220 nm. Calibration curves
60 were linear between 0.01 – 10 µg/mL, R² > 0.9991 with a lower limit of quantification 60 ng/mL in
61 plasma. Quantification of the samples analyzed was performed using standards diluted in a 90:10
62 Solvent A:Solvent B mixture, where each standard was injected 3 times, and quality control standards
63 were injected after every 10th injection performed (percent error < 11.8%).

64

65 Part B: PBPK modeling and simulations

66 List of tables

67

68 **Table B-SI** Two-compartment-model parameters for paracetamol performance following intravenous
69 administration of 168 mg of paracetamol to six healthy male beagles. Pharmacokinetic analysis was
70 performed using the PKPlus™ tool within the GastroPlus™ platform..... 6

71 **Table B-SII** One-compartment-model parameters for ibuprofen performance following intravenous
72 administration of 140 mg of ibuprofen to six healthy male beagles. Pharmacokinetic analysis was
73 performed using the PKPlus™ tool within the GastroPlus™ platform..... 6

74 **Table B-SIII** Input parameters in the canine PBPK model for paracetamol..... 7

75 **Table B-SIV** Input parameters in the canine PBPK model for ibuprofen..... 8

76 **Table B-SV** One-factor-at-a-time parameter sensitivity analysis performed for the paracetamol beagle
77 model (10 kg male beagle physiology): parameters, baseline values (value applied in the model) and
78 ranges for the parameters tested..... 9

79 **Table B-SVI** One-factor-at-a-time parameter sensitivity analysis performed for the ibuprofen beagle
80 model (10 kg male beagle physiology): parameters, baseline values (value applied in the model) and
81 ranges for the parameters tested..... 10

82 **Table B-SVII** Input parameters used to build the PBPK model for paracetamol..... 11

83 **Table B-SVIII** Input parameters used to build the human PBPK model for ibuprofen..... 12

84 **Table S-BIX** Fraction metabolized (fm) and enzyme maturation factors employed in the age-dependent
85 clearance estimations for ibuprofen..... 13

86

87 List of figures

88 **Figure B-S1** Observed and simulated plasma concentration-time profiles for paracetamol following
89 the i.v. administration of 168 mg of paracetamol to 6 beagles..... 15

90 **Figure B-S2** Observed and simulated paracetamol plasma concentrations in beagles (n=6) following
91 oral administration under fasted state conditions without (A) and with (B) gastric pH-lowering
92 pretreatment. 16

93 **Figure B-S3** Observed and simulated plasma concentration-time profiles for ibuprofen following i.v.
94 administration of 140 mg of ibuprofen to 6 beagles..... 17

95 **Figure B-S4** Observed and simulated ibuprofen plasma concentrations in beagles (n=6) following oral
96 administration under fasted state conditions without (A) and with (B) gastric pH-lowering
97 pretreatment. 18

98	Figure B-S5 Paracetamol parameter sensitivity analysis performed for effective permeability (upper	
99	panel) and gastric transit times (lower panel) in a beagle (male, 10 kg) under fasted state conditions,	
100	reference-meal fed state conditions, and infant-formula fed state conditions.	19
101	Figure B-S6 Paracetamol parameter sensitivity analysis performed for first pass metabolism changes	
102	between 6 - 24 % in a beagle (male, 10 kg) under fasted state conditions, reference-meal fed state	
103	conditions, and infant-formula fed state conditions.	19
104	Figure B-S7 Paracetamol simulations investigating sensitivity to gastric transit time (GTT) changes in	
105	beagles under the different dosing condition: fasted state conditions: range 0.1 h to 1 h (A),	
106	reference-meal fed state conditions: range 0.75 h to 3 h (B), and infant-formula fed state conditions:	
107	range 0.75 h to 3 h (C).	20
108	Figure B-S8 Paracetamol simulations investigating sensitivity to liver first pass metabolism (%)	
109	changes 6-24 % under fasted state conditions (A), reference-meal fed state conditions (B), and	
110	infant-formula fed state conditions (C).	21
111	Figure B-S9 Ibuprofen parameter sensitivity analysis performed for effective permeability (upper	
112	panel), duodenal pH (middle panel) and gastric transit times (lower panel) in a beagle (male, 10 kg)	
113	under fasted state conditions, reference-meal fed state conditions, and infant-formula fed state	
114	conditions.	22
115	Figure B-S10 Ibuprofen parameter sensitivity analysis performed for first pass metabolism changes	
116	between 10 - 30 % in a beagle (male, 10 kg) under fasted state conditions, reference-meal fed state	
117	conditions, and infant-formula fed state conditions.	22
118	Figure B-S11 Ibuprofen simulations investigating sensitivity to gastric transit time (GTT) changes	
119	under fasted state conditions: range 0.1 h to 1 h (A), reference-meal fed state conditions: range 0.1 h	
120	to 2.2 h (B), and infant-formula fed state conditions: range 0.1 h to 2.2 h (C).	23
121	Figure B-S12 Ibuprofen simulations investigating sensitivity to liver first pass metabolism (%)	
122	changes 10-30 % under fasted state conditions (A), reference-meal fed state conditions (B), and	
123	under infant-formula fed state conditions (C).	24
124	Figure B-S13 Fold difference (simulated/observed) for AUC_{0-8h} , C_{max} , T_{max} (A, D), Average Fold Error	
125	(B, E), and Absolute Average Fold Error (C, F) calculated from the simulated paracetamol profiles	
126	with PBPK model based on human adult bioavailability data (closed symbols, (42)) or based on	
127	beagle bioavailability data (open symbols, present study).	25
128	Figure B-S14 Fold difference (simulated/observed) for AUC_{0-8h} , C_{max} , T_{max} (A, D), Average Fold Error	
129	(B, E), and Absolute Average Fold Error (C, F) calculated from the mean simulated ibuprofen profiles	
130	with PBPK model based on human adult bioavailability data (closed symbols, (45)) or based on	
131	beagle bioavailability data (open symbols, present study).	26

132 **Table B-SI** Two-compartment-model parameters for paracetamol performance following intravenous
 133 administration of 168 mg of paracetamol to six healthy male beagles. Pharmacokinetic analysis was
 134 performed using the PKPlus™ tool within the GastroPlus™ platform.

Parameter	Mean Profile	Mean values ± SD
Clearance, CL (L/h)	12.66	13.13 ± 0.99
Volume of distribution in the central compartment, V _c (L/kg)	1.03	1.01 ± 0.09
Elimination half-life, t _{1/2} (h)	7.95	5.26 ± 2.24
k ₁₂ h ⁻¹	0.214	0.185 ± 0.062
K ₂₁ h ⁻¹	0.104	0.175 ± 0.060
Volume of distribution in the second compartment, V ₂ (L/kg)	2.115	1.29 ± 0.88

135

136

137 **Table B-SII** One-compartment-model parameters for ibuprofen performance following intravenous
 138 administration of 140 mg of ibuprofen to six healthy male beagles. Pharmacokinetic analysis was
 139 performed using the PKPlus™ tool within the GastroPlus™ platform.

Parameter	Mean Profile	Mean values ± SD
Clearance, CL (L/h)	0.478	0.479 ± 0.049
Volume of distribution in the central compartment, V _c (L/kg)	0.146	0.148 ± 0.022
Elimination half-life, t _{1/2} (h)	2.19	2.20 ± 0.29

140

141 **Table B-SIII** Input parameters in the canine PBPK model for paracetamol.

Parameter		Source
Physicochemical properties		
Molecular weight (g/mol)	151.2	(4–6)
Compound type	Monoprotic weak acid	
pKa	9.45 (acidic)	
logP	0.51	
Reference solubility in water (mg/mL)	14	(4)
Absorption		
Model	ACAT	GastroPlus™
Effective permeability, human (cm/s ×10 ⁴)	3.897	Calculated based on references (7–9)
Effective permeability, dog (cm/s ×10 ⁴)	10.39	Scaled from human GastroPlus™ (10)
Dissolution model	Johnson	GastroPlus™
Drug particle radius (µm)	25	Default GastroPlus™
Particle density (g/mL)	1.2	
Mean precipitation time (s)	900 ^a	
Diffusion coefficient (cm ² /s × 10 ⁵)	1.109	ADMET Predictor within GastroPlus™ (10,11)
Absorption scale factor (ASF) estimation	Opt LogD Model SA/V 6.1	GastroPlus™ (10)
Compartmental PK model (based on i.v. dosing)		
Fraction unbound (dogs), fu ^b	0.664	ADMET Predictor within GastroPlus™ (10,11)
Blood-plasma ratio (dogs)	1.01	
Clearance, CL (L/h)	12.66	2-compartment-model fit to the mean i.v. profile using the PKPlus™ tool within GastroPlus™
Volume of distribution in the central compartment, V _c (L/kg)	1.03	
Elimination half-life, t _{1/2} (h)	7.95	
k ₁₂ h ⁻¹	0.214	
K ₂₁ h ⁻¹	0.104	
Volume of distribution in the second compartment, V ₂ (L/kg)	2.115	

142 ^a default value was used for precipitation time due to drug high solubility and lack of model
143 sensitivity for this parameter; ^b adjusted fu,p option used within simulations; no bile salt
144 solubilization was assumed for paracetamol due to its high aqueous solubility.

145 **Table B-SIV** Input parameters in the canine PBPK model for ibuprofen.

Parameter		Source
Physicochemical properties		
Molecular weight (g/mol)	206.3	(12)
pKa	4.42 (acidic)	(13)
Compound type	Monoprotic acid	
clogP ^a	3.65	Predicted GastroPlus™
Reference solubility (mg/mL)	0.038	(14)
Aqueous solubility in mg/mL (pH)	0.038 (1.0)	
	0.043 (3.0)	
	0.084 (4.5)	
	0.685 (5.5)	
	3.37 (6.8)	
	3.44 (7.4)	
Absorption		
Model	ACAT™	GastroPlus™ (15)
Effective permeability, human (cm/s ×10 ⁴)	6.6	Calculated (8,16)
Effective permeability, dog (cm/s ×10 ⁴)	18.05	Scaled from human GastroPlus™ (10)
Solubility in biorelevant media (mg/mL)		In house data
Level III FaSSGF	0.048	
Level II FaSSIF	1.953	
Level II FeSSIF-V2	2.290	
Bile salt-solubilization ratio	1.4×10 ³	Estimated in GastroPlus™
Dissolution model	Johnson	GastroPlus™ (15)
Particle radius (µm)	25	Default GastroPlus™
Particle density (g/mL)	1.2	
Mean precipitation time (s) ^b	900	
Diffusion coefficient (cm ² /s × 10 ⁵)	0.939	ADMET Predictor within GastroPlus™ (10,11)
Absorption scale factor (ASF) estimation	Opt LogD Model SA/V 6.1	GastroPlus™ (10)
Compartmental PK model (based on i.v. dosing)		
Fraction unbound, fu ^c	0.0586	ADMET Predictor within GastroPlus™ (10,11)
Blood-plasma ratio	0.7	
Clearance, CL (L/h)	0.478	1-compartment-model fit to the mean i.v. profile using the PKPlus™ tool within GastroPlus™
Volume of distribution in the central compartment, Vc (L/kg)	0.146	
Elimination half-life, t _{1/2} (h)	2.19	

146 ^a calculated/predicted logP (octanol/water) by GastroPlus™, experimental logP range 3.23-4.13
 147 (13,17–19); ^b default value was used for precipitation time due to drug high solubility at intestinal pH
 148 and lack of model sensitivity for this parameter (drug is a weak acid, no precipitation occurs during
 149 transfer from stomach to duodenum); ^c adjusted fu,p option used within simulations
 150

151 **Table B-SV** One-factor-at-a-time parameter sensitivity analysis performed for the paracetamol beagle
 152 model (10 kg male beagle physiology): parameters, baseline values (value applied in the model) and
 153 ranges for the parameters tested.

Parameter	Baseline	Lower range limit	Upper range limit
All prandial/dosing conditions			
Effective permeability (cm/s ×10 ⁴)	10.39	1.039	35.0
Diffusion coefficient (cm ² /s ×10 ⁵)	1.109	0.111	1.109
Particle size (µm)	25	2.5	100
Precipitation time (s)	900	90	9000
Dose volume (mL)	24	2	35
Small intestinal length (cm)	150	75	300
Small intestinal radius (cm)	0.5	0.25	1.0
Small intestinal transit time (h)	1.82	0.91	3.64
Fraction of small intestinal fluid in fasted state (%)	40	20	80
Duodenal pH	6.2	0.5	8.0
Jejunal pH	6.2	0.5	8.0
Liver first pass effect (%)	12	6	25
Fasted state conditions			
Gastric pH	1.6	0.5	8.0
Gastric volume (mL)	51	25.5	102
Gastric transit time (h)	0.5	0.1	1.0
Reference-meal/Infant-formula fed state conditions			
Gastric pH	5.0	0.5	8
Gastric volume (mL)	1000	500	2000
Gastric transit time (h), Zero order gastric emptying	1.5	0.75	3.0

154

155

156 **Table B-SVI** One-factor-at-a-time parameter sensitivity analysis performed for the ibuprofen beagle
 157 model (10 kg male beagle physiology): parameters, baseline values (value applied in the model) and
 158 ranges for the parameters tested.

Parameter	Baseline	Lower range limit	Upper range limit
All prandial/dosing conditions			
Effective permeability (cm/s ×10 ⁴)	18.05	1.0	36.1
Bile salt solubilization ratio	1.4×10 ³	1.0×10 ³	2.8×10 ³
Diffusion coefficient (cm ² /s ×10 ⁵)	0.939	0.47	1.0
Reference solubility (mg/mL)	0.038	0.0038	0.076
Particle size (µm)	25	2.5	100
Precipitation time (s)	900	90	9000
Dose volume (mL)	24	2	35
Small intestinal length (cm)	150	75	300
Small intestinal radius (cm)	0.5	0.25	1.0
Small intestinal transit time (h)	1.82	0.91	3.64
Fraction of small intestinal fluid in fasted state (%)	40	20	80
Duodenal pH	6.2	0.5	8.0
Jejunal pH	6.2	0.5	8.0
Liver first pass effect (%)	22	10	35
Fasted state conditions			
Gastric pH	1.6	0.5	8.0
Gastric volume (mL)	51	25.5	102
Gastric transit time (h)	0.25	0.1	1.0
Reference-meal/Infant-formula fed state conditions			
Gastric pH	5.0	0.5	8
Gastric volume (mL)	1000	500	2000
Gastric transit time (h), Zero order gastric emptying	1.1	0.1	2.2

159

160 **Table B-SVII** Input parameters used to build the PBPK model for paracetamol

Parameter		Source
Physicochemical properties		
Molecular weight (g/mol)	151.2	(4–6)
Compound type	Monoprotic weak acid	(4–6)
pKa	9.45 (acidic)	(4–6)
logP ^a	0.51	(4–6)
Reference solubility in water (mg/mL)	14	(4)
Absorption		
Model	ACAT	GastroPlus™
Effective permeability, human (cm/s ×10 ⁴)	3.897	Calculated based on (7–9)
Dissolution model	Johnson	GastroPlus™
Drug particle radius (μm)	25	Default GastroPlus™
Absorption scale factor (ASF) estimation	Opt LogD Model SA/V 6.1	GastroPlus™ (10)
Distribution		
Fraction unbound, fu	0.82	(11)
Blood-plasma ratio	1.09	(20)
Predicted Vss (L/kg) ^b	0.86	Predicted using the Lukacova, Rodgers and Rowland method (21–23)
Clearance		
<i>In vivo</i> clearance (L/h)	19.7	(24)
Enzyme kinetics		
	Km (μM)	Vmax (pmol/min/mg microsomal protein)
CYP1A2 ^c	220	30.78
CYP2C9 ^c	660	8.42
CYP2C19 ^c	2000	25.53
CYP2D6 ^c	440	5.62
CYP2E1 ^c	4020	76.97
CYP3A4 ^c	130	57.16
UGT1A1 ^d	5500	6102.67
UGT1A9 ^d	9200	10208.11
UGT2B15 ^d	23000	34045.84
SULT1A1 ^e	2400	1374.06
SULT1A3 ^e	1500	202.89
SULT1E1 ^e	1900	146.22
SULT2A1 ^e	3700	828.35

161 ^a to achieve the benchmark Vss values observed *in vivo*, initially logP value of 1.2 was used for the
 162 calculation of the tissue partitioning coefficients (Kp) (6); measured logP value 0.51 was used thought
 163 simulations; ^b Predicted volume of distribution at steady state (Vss); ^c Cytochrome P450 (CYP)
 164 isoenzyme, ^d UDP-glucuronosyltransferase (UGT) isoenzyme, and ^e cytosolic sulfotransferases (SULT)
 165 isoenzyme contributing to paracetamol metabolism
 166

167

168 **Table B-SVIII** Input parameters used to build the human PBPK model for ibuprofen

Parameter		Source
Physicochemical properties		
Molecular weight (g/mol)	206.3	(12)
pKa	4.42 (acidic)	(13)
Compound type	Monoprotic weak acid	
clogP*	3.65	Predicted GastroPlus™
Reference solubility (mg/mL)	0.038	(14)
Aqueous solubility in mg/mL (pH)	0.038 (1.0)	(14)
	0.043 (3.0)	
	0.084 (4.5)	
	0.685 (5.5)	
	3.37 (6.8)	
	3.44 (7.4)	
Absorption		
Model	ACAT™	
Effective permeability, human (cm/s ×10 ⁴)	6.6	Calculated based on (8,16)
Solubility in biorelevant media (mg/mL)		In house data
Level III FaSSGF	0.048	
Level II FaSSIF	1.953	
Level II FeSSIF-V2	2.290	
Dissolution model	Johnson	GastroPlus™, (15)
Particle size, radius (µm)	25	Default GastroPlus™
Absorption scale factor (ASF) estimation	Opt LogD Model SA/V 6.1	GastroPlus™ (10)
Distribution		
Fraction unbound, fu	0.0155	(28)
Blood-plasma ratio	1.55	(29)
Vss (L/kg) ^a	0.11	Predicted using the Lukacova, Rodgers and Rowland method (21,23)
Clearance		
Clearance (L/h)	3.81	Adjusted based on healthy adults Pavliv <i>et al.</i> (30)

169 *calculated/predicted logP (octanol/water) by GastroPlus™, experimental logP range 3.23-4.13
 170 (13,17–19)

171

172 Clearance scaling

173 The hepatic intrinsic clearance ($CL_{int,u,H}$) parameter was incorporated as whole organ clearance in the
 174 model and was calculated according to the well-stirred clearance model (6,10,31), i.e. Eq. S1.

$$175 \quad CL_{int,u,H} = \frac{Q_{H,B} \times CL_H}{F_{u,p} \times (Q_{H,B} - CL_H/B:P)} \quad \text{Eq. S1}$$

176 where $Q_{H,B}$ is the hepatic blood flow (L/h), f_u is the fraction of drug unbound in plasma, CL_H is the
 177 hepatic clearance observed *in vivo* (L/h) and B:P denotes the blood to plasma concentration ratio of
 178 the drug (Table B-SVII).

179
 180 Although the two ibuprofen enantiomers exhibit quantitatively different metabolic contributions of
 181 the different CYP and UGT isoenzymes, the proportions of (S)-ibuprofen metabolized by the different
 182 isoenzymes was considered in the present modeling exercise of the racemic ibuprofen. This
 183 simplification was adopted to facilitate clearance scaling to paediatrics and because the (R)-
 184 enantiomer undergoes extensive systemic inversion to the S-enantiomer (17,32). Pre-systemic
 185 inversion of (R)- to (S)- ibuprofen has been considered negligible in literature (32), as studies
 186 investigating intravenous and oral (R)-ibuprofen administration in adults revealed no pharmacokinetic
 187 differences between the two administration routes (33–35). Based on urinary recovery data of
 188 ibuprofen (metabolites) in adults (36,37), fraction metabolized (fm) values for CYP2C9, CYP2C8,
 189 UGT1A9, and UGT2B7 were estimated and reported in Table S-BVIII.

190 **Table S-BIX** Fraction metabolized (fm) and enzyme maturation factors employed in the age-dependent
 191 clearance estimations for ibuprofen.

Metabolizing enzyme	Fraction metabolized (fm)		Maturation factor (MF) ^a		
	Adult/Paediatric	Source	Infant (12 - 24 months)	Child (6-year-old)	Source
CYP2C9	0.8460	(36,37)	0.90	1.00	(38)
CYP2C8	0.0059	(36,37)	0.99	1.00	(38)
UGT1A9	0.1502	(36,37)	1.25	1.16	(39)
UGT2B7	0.0038	(36,37)	0.87	2.16	(39)

192 ^a Maturation factor calculated from enzyme abundance/activity in paediatric microsomes vs. adults
 193

194 Furthermore, maturation processes in paediatrics were considered for age-dependent ibuprofen
 195 clearance estimations, based on their crucial role for capturing drug clearance at young ages, i.e.
 196 younger children and infants (38,40). The approach applied in the present study is commonly
 197 implemented in PBPK modeling routines (38,40,41). Clearance scaling was performed based on an
 198 allometric scaling factor of 0.75 (ASF) and a maturation factor (MF_{age}) for the involved metabolizing
 199 enzymes as shown in Eq. S2 and Eq. S3, respectively.

200
$$CL_{paediatrics} = CL_{adult} \times \left(\frac{BW_{paediatrics}}{BW_{adult}} \right)^{0.75} \times MF_{age} \quad \text{Eq. S2}$$

201 where $CL_{paediatrics}$ is the clearance in the paediatric population representative (L/h), CL_{adult} is the
202 clearance in adults (L/h), $BW_{paediatrics}$ and BW_{adult} are the body weights of the paediatric and adult
203 representatives, respectively, and the MF_{age} is the maturation factor for the specific age (Eq. S3) .

204
$$MF_{age} = a \times MF_{CYP2C9} + b \times MF_{CYP2C8} + c \times MF_{UGT1A9} + d \times MF_{UGT2B7} \quad \text{Eq. S3}$$

205 where a, b, c, and d are the fm(CYP2C9), fm(CYP2C8), fm(UGT1A9), and fm(UGT2B7), respectively;
206 MF_{CYP2C9} , MF_{CYP2C8} , MF_{UGT1A9} , and MF_{UGT2B7} denote the relative isoenzyme activity at the relevant
207 paediatric age vs. the adult activity for CYP2C9, CYP2C8, UGT1A9, and UGT2B7, respectively. Values
208 employed in the present study are reported in Table S-BVIII. MPPGL ontogeny was not taken into
209 consideration in the present model

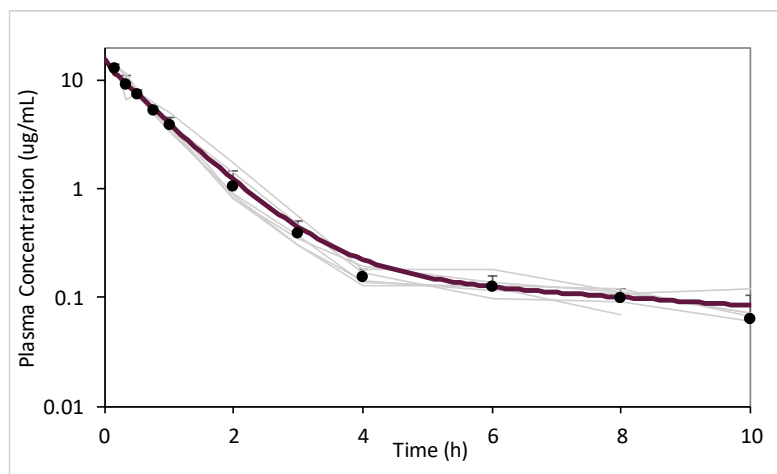


Figure B-S1 Observed and simulated plasma concentration-time profiles for paracetamol following the i.v. administration of 168 mg of paracetamol to 6 beagles. Mean observed plasma concentrations and standard deviations are depicted with filled circles and error bars, individual profiles with grey lines; simulated mean profile with a purple bold line.

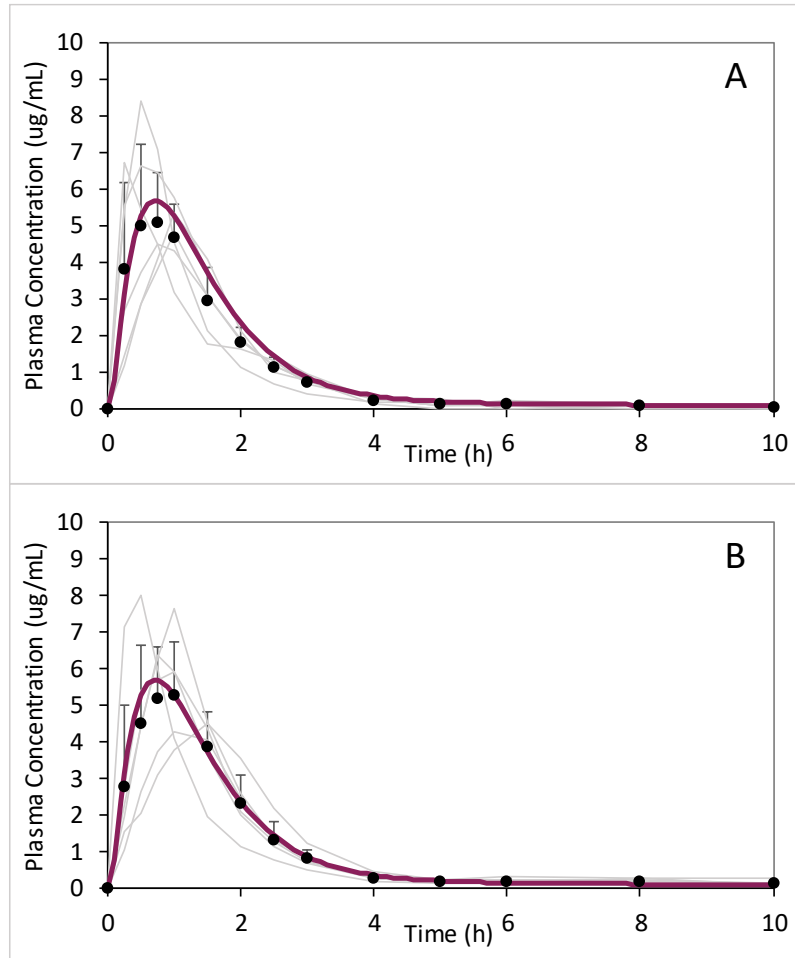


Figure B-S2 Observed and simulated paracetamol plasma concentrations in beagles (n=6) following oral administration under fasted state conditions without (A) and with (B) gastric pH-lowering pretreatment. For both simulations gastric transit time of 0.5 h was employed. Simulations without pretreatment (A) resulted in AFE / AAFE of 1.307 / 1.349, while simulations of drug performance with pretreatment resulted in AFE / AAFE of 0.960 / 1.195. Mean observed plasma concentrations and standard deviations are depicted with filled circles and error bars, individual profiles are presented with grey lines, simulated mean profile is presented with a purple bold line.

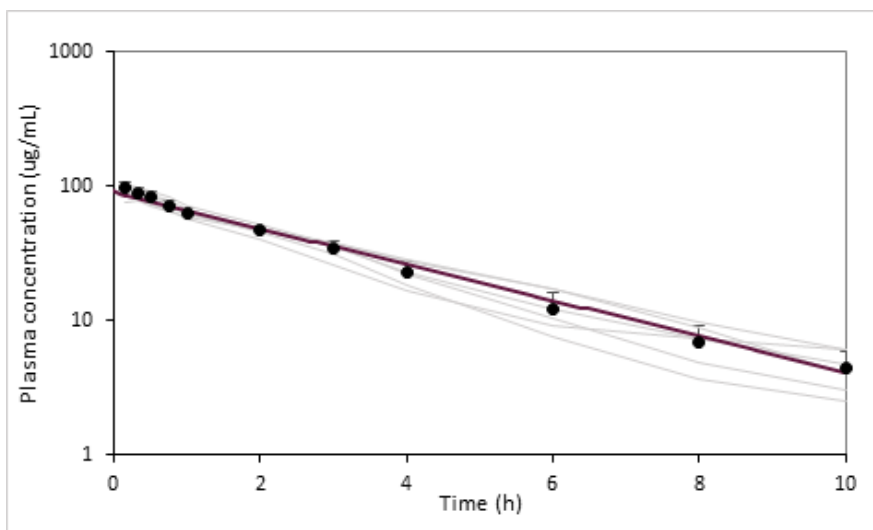


Figure B-S3 Observed and simulated plasma concentration-time profiles for ibuprofen following i.v. administration of 140 mg of ibuprofen to 6 beagles. Mean observed plasma concentrations and standard deviations are depicted with filled circles and error bars; individual profiles grey lines; simulated mean profile with a purple bold line.

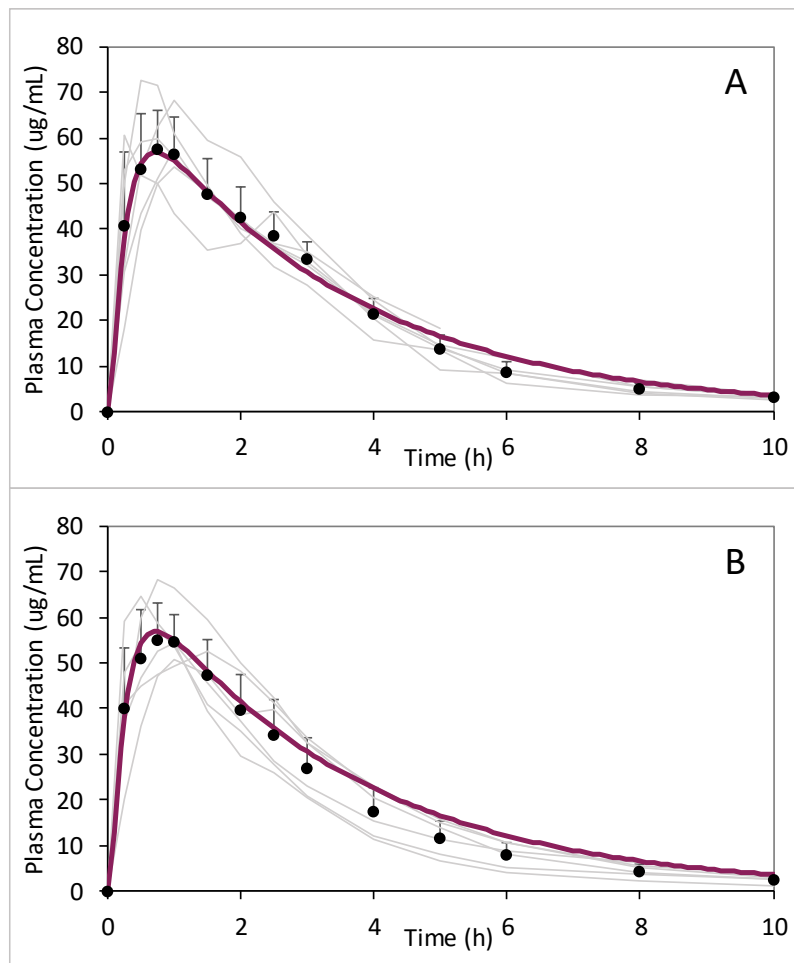


Figure B-S4 Observed and simulated ibuprofen plasma concentrations in beagles (n=6) following oral administration under fasted state conditions without (A) and with (B) gastric pH-lowering pretreatment. For both simulations gastric transit time of 0.25 h was employed. Simulations without pretreatment (A) resulted in AFE / AAFE of 1.049 / 1.099, while simulations of drug performance with pretreatment resulted in AFE / AAFE of 1.162 / 1.172. Mean observed plasma concentrations and standard deviations are depicted with filled circles and error bars, individual profiles are presented with grey lines, simulated mean profile is presented with a purple bold line.

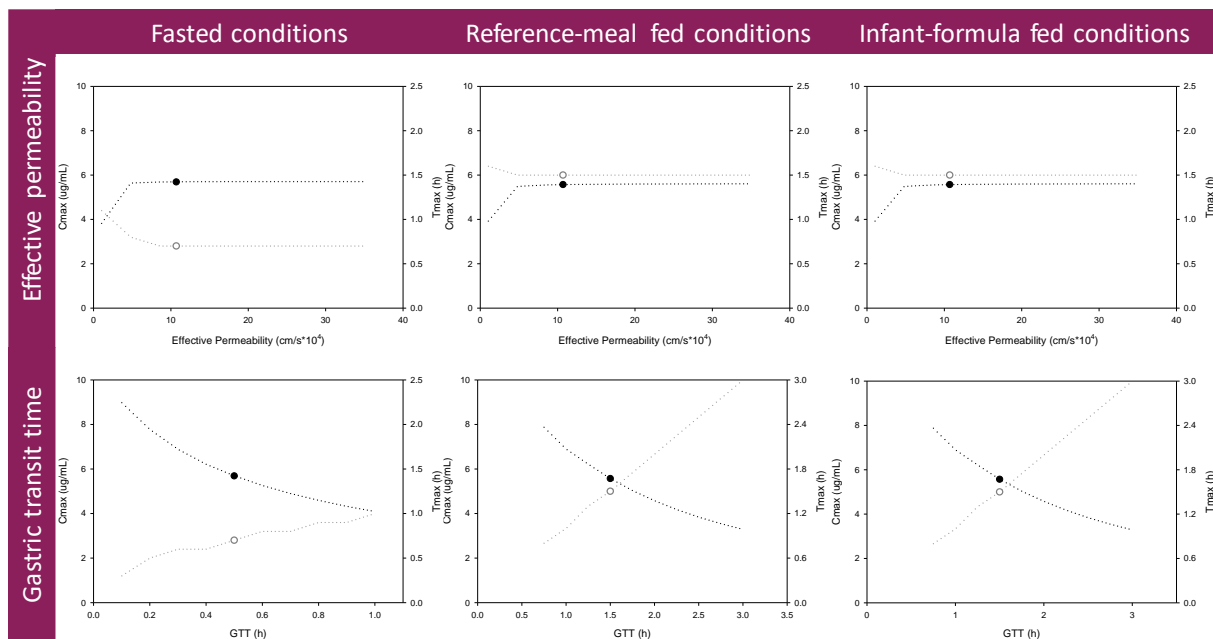


Figure B-S5 Paracetamol parameter sensitivity analysis performed for effective permeability (upper panel) and gastric transit times (lower panel) in a beagle (male, 10 kg) under fasted state conditions, reference-meal fed state conditions, and infant-formula fed state conditions. Black lines depict C_{max} values (left Y-axis) and grey lines depict T_{max} values (right Y-axis). Symbols denote the parameter value (baseline) employed in the performed beagle simulations.

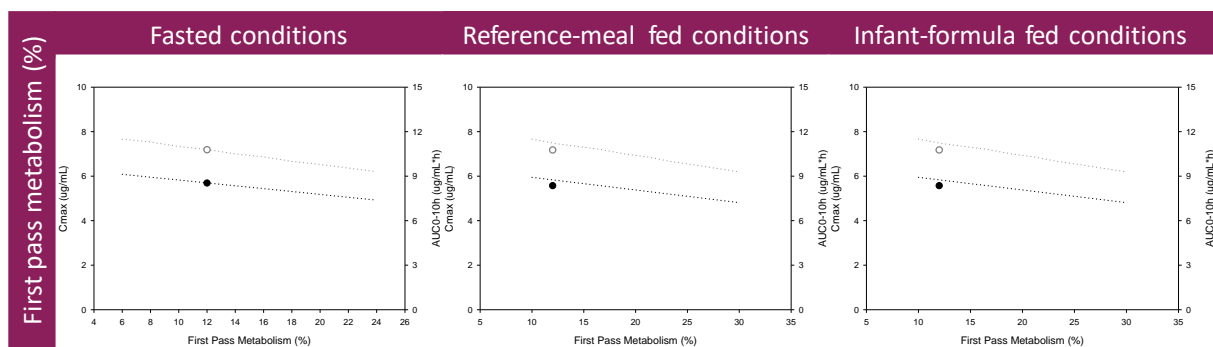


Figure B-S6 Paracetamol parameter sensitivity analysis performed for first pass metabolism changes between 6 - 24 % in a beagle (male, 10 kg) under fasted state conditions, reference-meal fed state conditions, and infant-formula fed state conditions. Black lines depict C_{max} values (left Y-axis) and grey lines depict AUC_{0-10h} values (right Y-axis). Symbols denote the parameter value (baseline) employed in the performed beagle simulations.

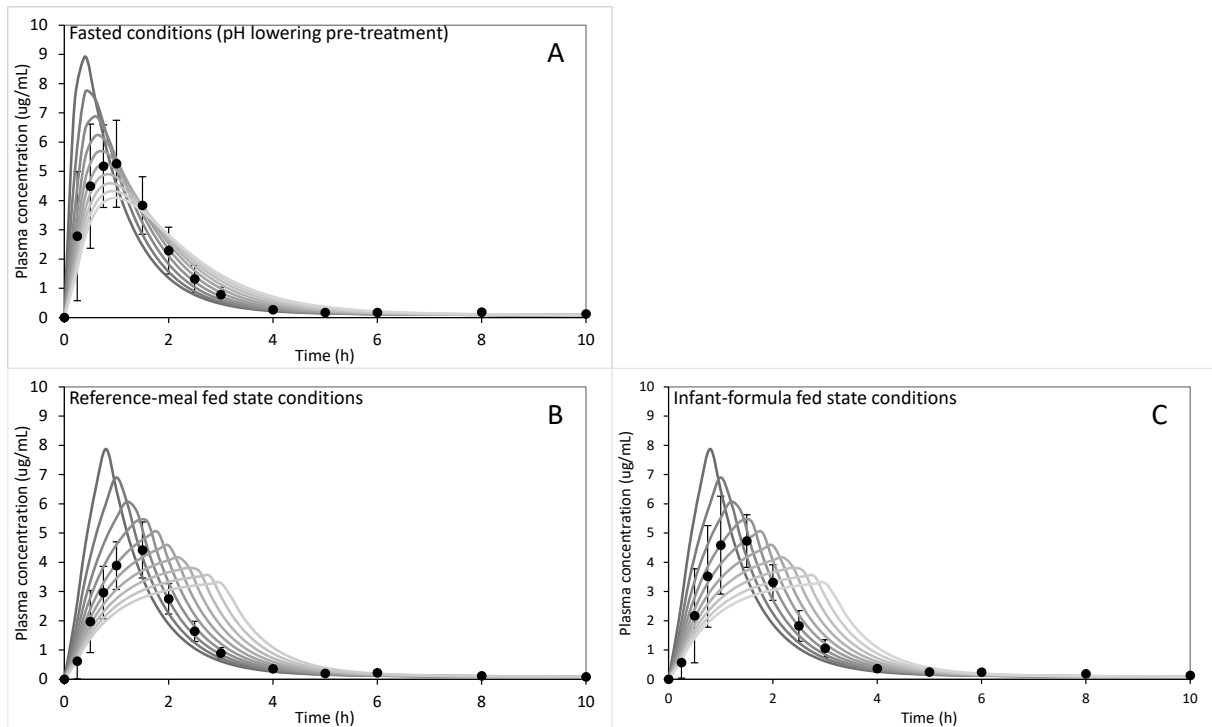


Figure B-S7 Paracetamol simulations investigating sensitivity to gastric transit time (GTT) changes in beagles under the different dosing condition: fasted state conditions: range 0.1 h to 1 h (A), reference-meal fed state conditions: range 0.75 h to 3 h (B), and infant-formula fed state conditions: range 0.75 h to 3 h (C). Grey lines denote simulated plasma concentration-time profiles, with dark to light color gradient denoting rapid to slow GTT values (10 steps), symbols and error bars denote mean and standard deviation observed in the canine study (n=6 Beagles).

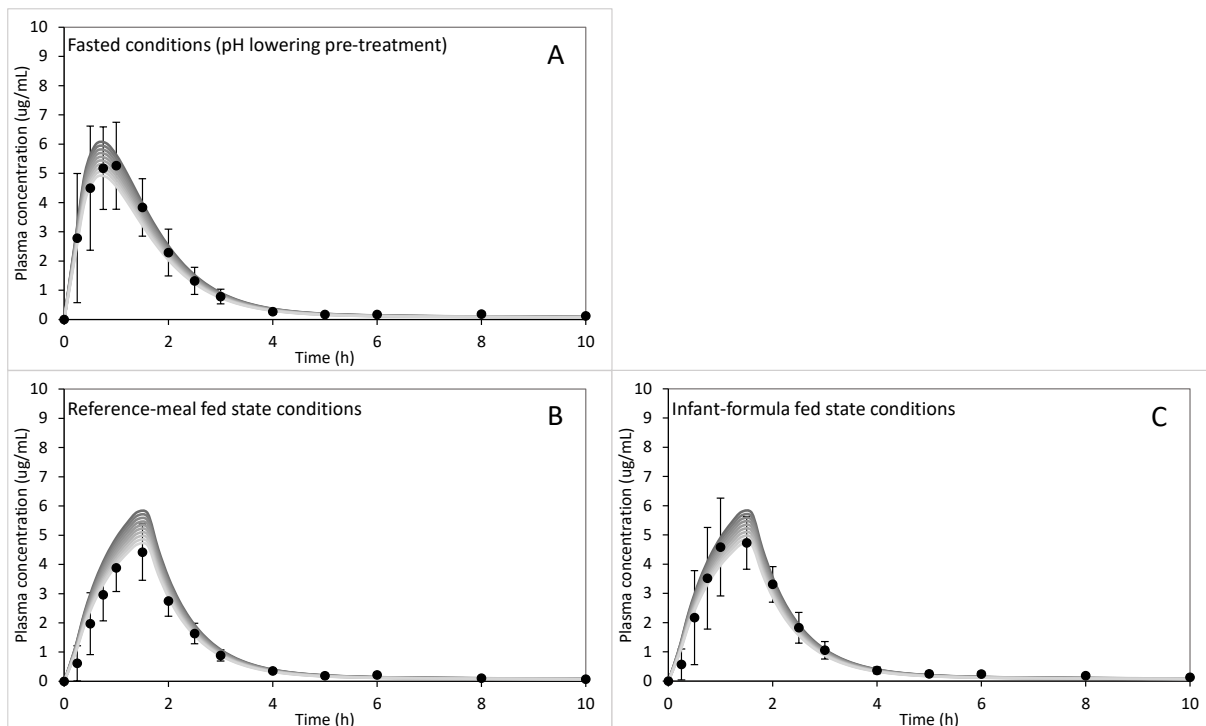


Figure B-S8 Paracetamol simulations investigating sensitivity to liver first pass metabolism (%) changes 6-24 % under fasted state conditions (A), reference-meal fed state conditions (B), and infant-formula fed state conditions (C). Grey lines denote simulations, with dark to light color gradient denoting low to high first pass metabolism values (10 steps), symbols and error bars denote mean and standard deviations observed in the *in vivo* study in beagles.

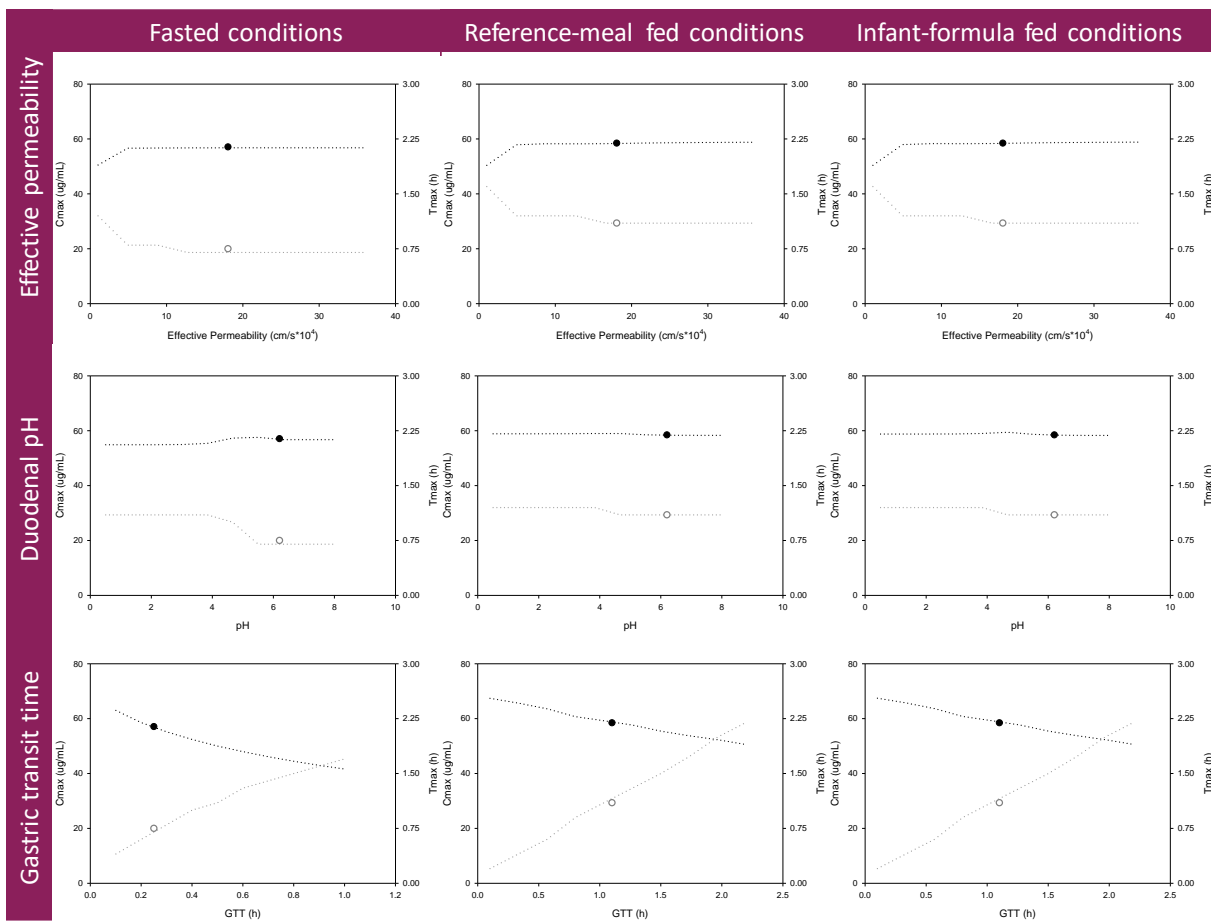


Figure B-S9 Ibuprofen parameter sensitivity analysis performed for effective permeability (upper panel), duodenal pH (middle panel) and gastric transit times (lower panel) in a beagle (male, 10 kg) under fasted state conditions, reference-meal fed state conditions, and infant-formula fed state conditions. Black lines depict C_{max} values (left Y-axis) and grey lines depict T_{max} values (right Y-axis). Symbols denote the parameter value (baseline) employed in the performed beagle simulations.

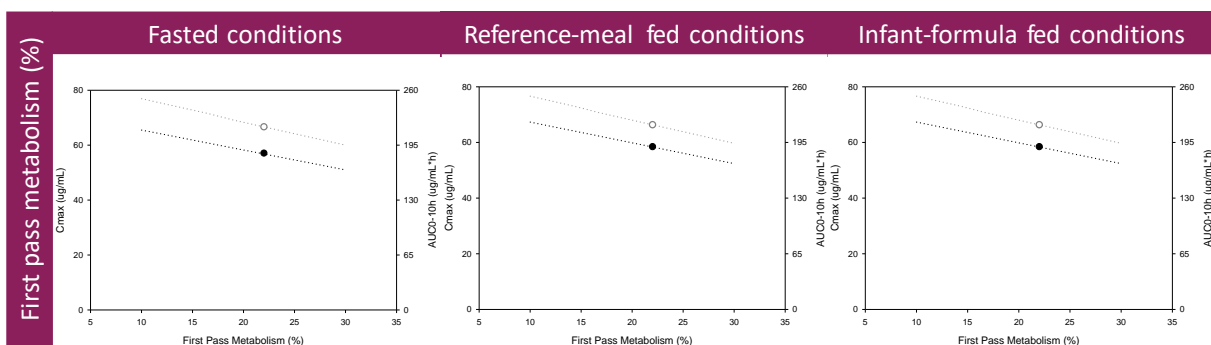


Figure B-S10 Ibuprofen parameter sensitivity analysis performed for first pass metabolism changes between 10 - 30 % in a beagle (male, 10 kg) under fasted state conditions, reference-meal fed state conditions, and infant-formula fed state conditions. Black lines depict C_{max} values (left Y-axis) and grey lines depict AUC_{0-10h} values (right Y-axis). Symbols denote the parameter value (baseline) employed in the performed beagle simulations.

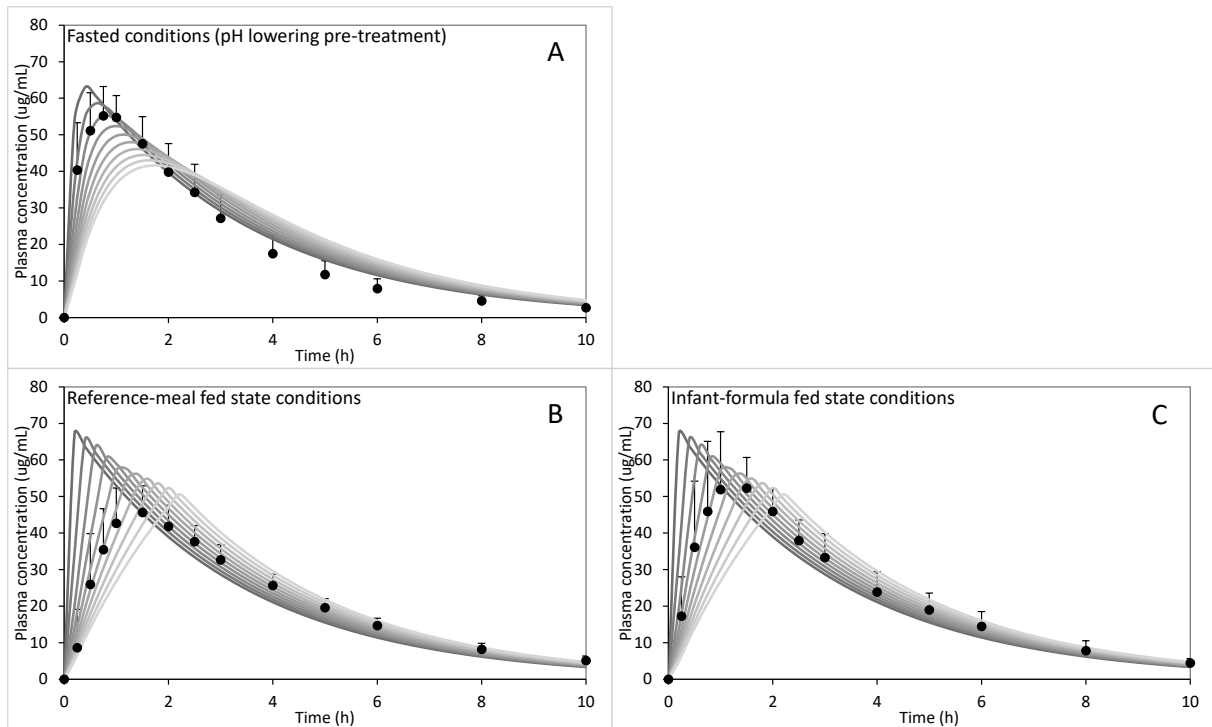


Figure B-S11 Ibuprofen simulations investigating sensitivity to gastric transit time (GTT) changes under fasted state conditions: range 0.1 h to 1 h (A), reference-meal fed state conditions: range 0.1 h to 2.2 h (B), and infant-formula fed state conditions: range 0.1 h to 2.2 h (C). Grey lines denote simulated plasma concentration-time profiles, with dark to light color gradient denoting rapid to slow GTT values (10 steps), symbols and error bars denote mean concentrations and standard deviations observed in the canine study.

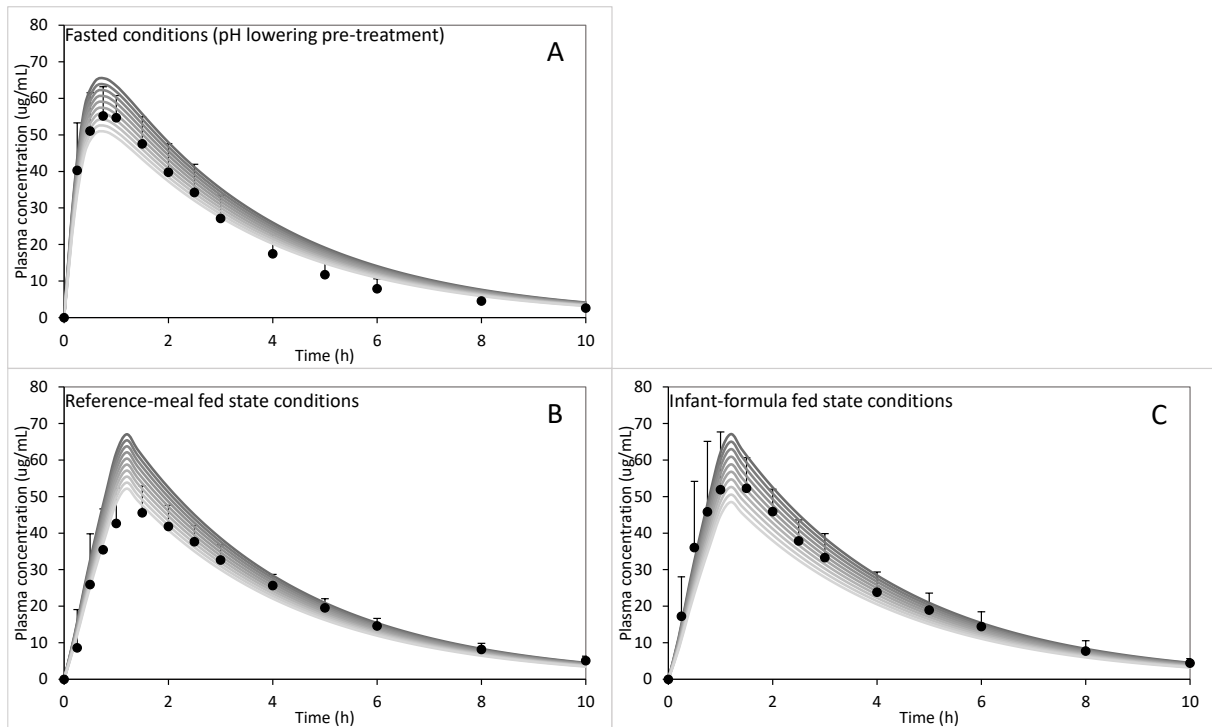


Figure B-S12 Ibuprofen simulations investigating sensitivity to liver first pass metabolism (%) changes 10-30 % under fasted state conditions (A), reference-meal fed state conditions (B), and under infant-formula fed state conditions (C). Grey lines denote simulations, with dark to light color gradient denoting low to high first pass metabolism values (10 steps), symbols and error bars denote mean and standard deviations observed in the *in vivo* study in beagles.

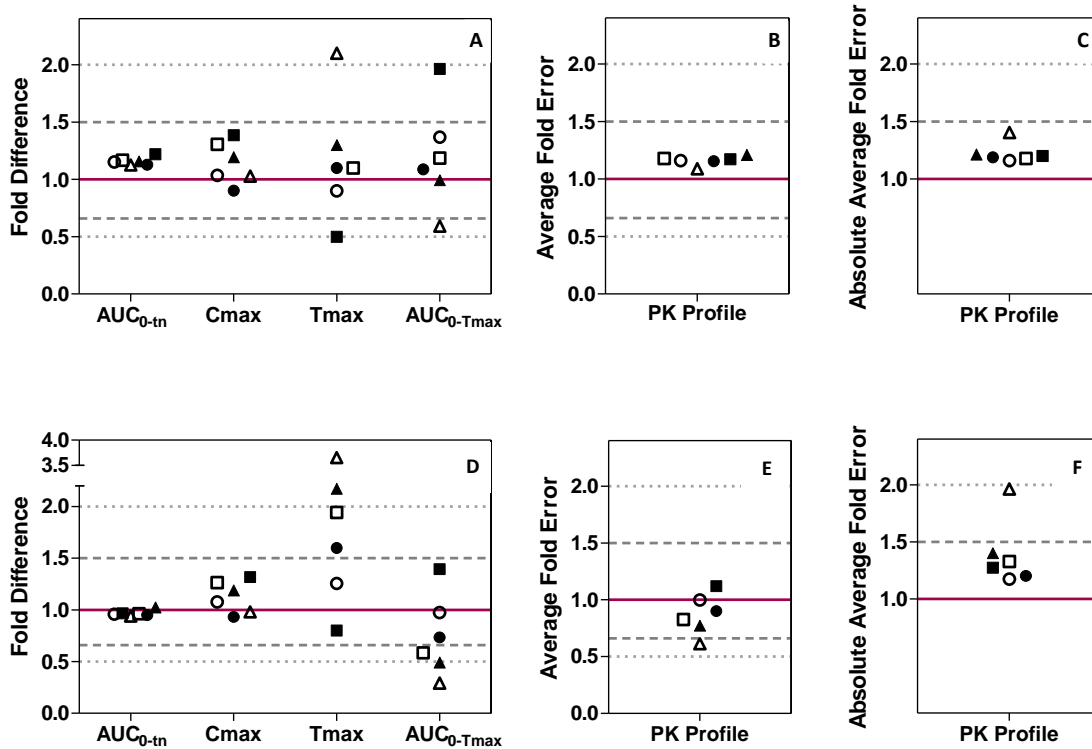


Figure B-S13 Fold difference (simulated/observed) for AUC_{0-8h} , C_{max} , T_{max} (A, D), Average Fold Error (B, E), and Absolute Average Fold Error (C, F) calculated from the simulated paracetamol profiles with PBPK model based on human adult bioavailability data (closed symbols, (42)) or based on beagle bioavailability data (open symbols, present study). Upper panel (A, B, C) depicts model performance according to the study by Hopkins et al., 1990 (43) (study mean age 4 months); lower panel (D, E, F) study by Walson et al., 2013 (44) (study mean age 10 months). Adjusted fasted state conditions (circles), adjusted reference-meal fed state conditions (squares), and adjusted infant-formula fed state conditions (triangles). The solid line represents the line of unity, grey dashed lines 0.66-1.5 range indicating successful simulations, and grey dotted lines the 0.5-2 range indicating adequate simulations.

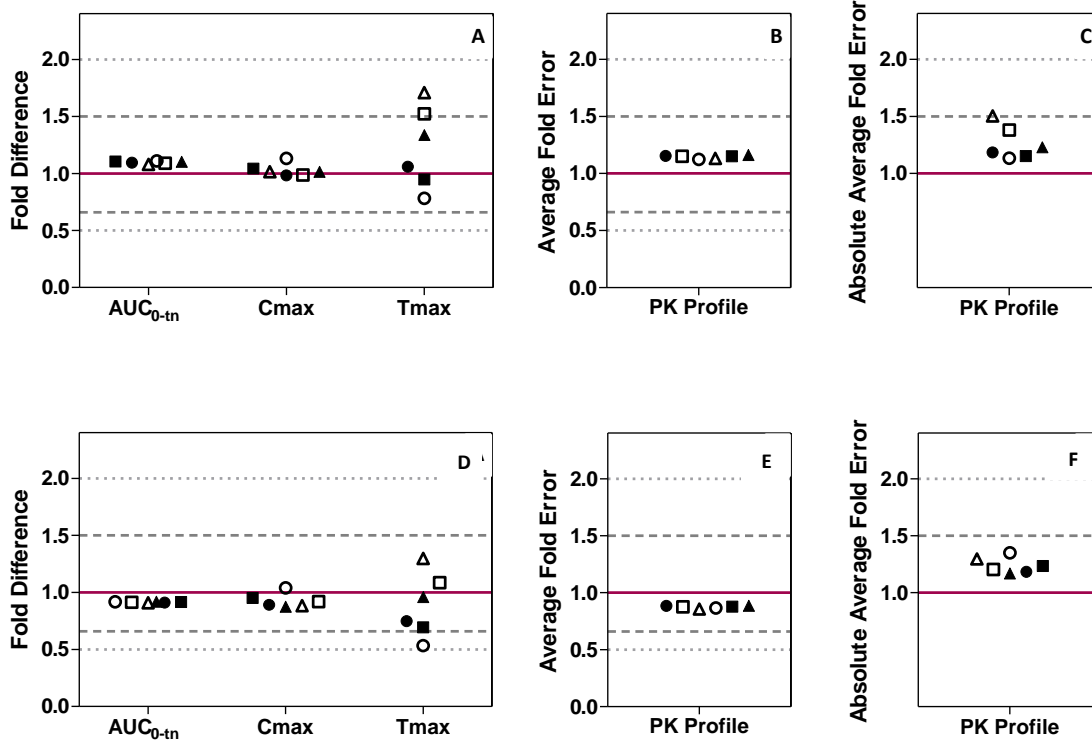


Figure B-S14 Fold difference (simulated/observed) for AUC_{0-8h} , C_{max} , T_{max} (A, D), Average Fold Error (B, E), and Absolute Average Fold Error (C, F) calculated from the mean simulated ibuprofen profiles with PBPK model based on human adult bioavailability data (closed symbols, (45)) or based on beagle bioavailability data (open symbols, present study). Upper panel (A, B, C) depicts model performance according to the study by Brown et al., 1992 (46) (study age range 0.3-12 years); lower panel (D, E, F) study by Walson et al., 1989 (47) (study age range 2-11 years). Adjusted fasted state conditions (circles), adjusted reference-meal fed state conditions (> 2.5 years) and adjusted reference-meal fed state conditions (< 2.5 years) and adjusted infant-formula fed state conditions (< 2.5 years) (triangles). The solid line represents the line of unity, grey dashed lines 0.66 -1.5 range indicating successful simulations, and grey dotted lines the 0.5-2 range indicating adequate simulations.

References

1. Vertzoni M V., Archontaki HA, Galanopoulou P. Development and optimization of a reversed-phase high-performance liquid chromatographic method for the determination of acetaminophen and its major metabolites in rabbit plasma and urine after a toxic dose. *J Pharm Biomed Anal.* 2003;32(3):487–93.
2. Lalande M, Wilson DL, MCGilveray IJ. Rapid high-performance in human plasma. *J Chromatogr B.* 1986;377:410–4.
3. Statelova M, Goumas K, Fotaki N, Holm R, Symillides M, Reppas C, et al. On the Design of Food Effect Studies in Adults for Extrapolating Oral Drug Absorption Data to Infants : an Exploratory Study Highlighting the Importance of Infant Food. *AAPS J.* 2020;22(6):1–11.
4. Kalantzi L, Reppas C, Dressman JB, Amidon GL, Junginger HE, Midha KK, et al. Biowaiver monographs for immediate release solid oral dosage forms: Acetaminophen (Paracetamol). *J Pharm Sci.* 2006;95(1):4–14.
5. Jiang X-L, Zhao P, Barrett JS, Lesko LJ, Schmidt S. Application of physiologically based pharmacokinetic modeling to predict acetaminophen metabolism and pharmacokinetics in children. *CPT pharmacometrics Syst Pharmacol.* 2013;2(August):e80.
6. Ladumor MK, Bhatt DK, Gaedigk A, Sharma S, Thakur A, Pearce RE, et al. Ontogeny of hepatic sulfotransferases and prediction of age-dependent fractional contribution of sulfation in acetaminophen metabolism. *Drug Metab Dispos.* 2019;47(8):818–31.
7. Johnson TN, Bonner JJ, Tucker GT, Turner DB, Jamei M. Development and application of a physiologically-based model of paediatric oral drug absorption. *Eur J Pharm Sci.* 2018;
8. Sun D, Lennernas H, Welage LS, Barnett JL, Landowski CP, Foster D, et al. Comparison of human duodenum and Caco-2 gene expression profiles for 12,000 gene sequences tags and correlation with permeability of 26 drugs. *Pharm Res.* 2002;19(10):1400–16.
9. Yamashita S, Furubayashi T, Kataoka M, Sakane T, Sezaki H, Tokuda H. Optimized conditions for prediction of intestinal drug permeability using Caco-2 cells. *Eur J Pharm Sci.* 2000;10(3):195–204.
10. SimulationsPlus Inc. GastroPlus Manual. 2020.
11. Strougo A, Eissing T, Yassen A, Willmann S, Danhof M, Freijer J. First dose in children: Physiological insights into pharmacokinetic scaling approaches and their implications in paediatric drug development. *J Pharmacokinet Pharmacodyn.* 2012;39(2):195–203.
12. Pharmacopoeia E. Ibuprofen. *Ph Eur.* 2008;7(1):2225–7.
13. Avdeef A, Berger CM, Brownell C. pH-metric solubility. 2: Correlation between the acid-base titration and the saturation shake-flask solubility-pH methods. *Pharm Res.* 2000;17(1):85–9.
14. Potthast H, Dressman JB, Junginger HE, Midha KK, Oeser H, Shah VP, et al. Biowaiver monographs for immediate release solid oral dosage forms: Ibuprofen. *J Pharm Sci.* 2005;94(10):2121–31.

15. Lu ATK, Frisella ME, Johnson KC. Dissolution Modeling: Factors Affecting the Dissolution Rates of Polydisperse Powders. *Pharm Res.* 1993;10(9):1308–14.
16. Yee S. In vitro permeability across Caco-2 cells (colonic) can predict in vivo (small intestinal) absorption in man - fact or myth. *Pharm Res.* 1997;14(6):763–6.
17. Cristofolletti R, Dressman JB. Use of Physiologically Based Pharmacokinetic Models Coupled with Pharmacodynamic Models to Assess the Clinical Relevance of Current Bioequivalence Criteria for Generic Drug Products Containing Ibuprofen. *J Pharm Sci.* 2014;103:3263–75.
18. Kasim NA, Whitehouse M, Ramachandran C, Bermejo M, Lennernäs H, Hussain AS, et al. Molecular Properties of WHO Essential Drugs and Provisional Biopharmaceutical Classification. *Mol Pharm.* 2004;1(1):85–96.
19. Avdeef A, Box KJ, Comer JEA, Gilges M, Hadley M, Hibbert C, et al. PH-metric log P 11 . pK a determination of water-insoluble drugs in organic solvent – water mixtures. *J Pharm Biomed Anal.* 1999;20:631–41.
20. Prescott L. Kinetics and metabolism of paracetamol and phenacetin. *Br J Clin Pharmacol.* 1980;10(2 S):291S-298S.
21. Rodgers T, Rowland M. Physiologically Based Pharmacokinetic Modelling 2: Predicting the Tissue Distribution of Acids, Very Weak Bases, Neutrals and Zwitterions. *J Pharm Sci.* 2005;95(6):1238–57.
22. Kohlmann P, Stillhart C, Kuentz M, Parrott N. Investigating Oral Absorption of Carbamazepine in Pediatric Populations. *AAPS J.* 2017;19(6):1864–77.
23. Lukacova V, Parrott NJ, Lave T, Fraczkiwicz G, Bolger MB. Role of fraction unbound in plasma in calculation of tissue:plasma partition coefficients. In: AAPS National meeting, Atlanta, November 15-20. 2008.
24. Clements J, Critchley J, Prescott L. The role of sulphate conjugation in the metabolism and disposition of oral and intravenous paracetamol in man. *Br J Clin Pharmacol.* 1984;18(4):481–5.
25. Laine JE, Auriola S, Pasanen M, Juvonen RO. Acetaminophen bioactivation by human cytochrome P450 enzymes and animal microsomes. *Xenobiotica.* 2009;39(1):11–21.
26. Mutlib AE, Goosen TC, Bauman JN, Williams JA, Kulkarni S, Kostrubsky S. Kinetics of acetaminophen glucuronidation by UDP-glucuronosyltransferases 1A1, 1A6, 1A9 and 2B15. Potential implications in acetaminophen-induced hepatotoxicity. *Chem Res Toxicol.* 2006;19(5):701–9.
27. Adjei AA, Gaedigk A, Simon SD, Weinshilboum RM, Leeder JS. Interindividual variability in acetaminophen sulfation by human fetal liver: Implications for pharmacogenetic investigations of drug-induced birth defects. *Birth Defects Res Part A - Clin Mol Teratol.* 2008;82(3):155–65.
28. Aarons L, Grennan DM, Siddiqui M. The binding of ibuprofen to plasma proteins. *Eur J Clin Pharmacol.* 1983;25(6):815–8.

29. Obach RS. Prediction of human clearance of twenty-nine drugs from hepatic microsomal intrinsic clearance data: An examination of in vitro half-life approach and nonspecific binding to microsomes. *Drug Metab Dispos.* 1999;27(11):1350–9.
30. Pavliv L, Voss B, Rock A. Pharmacokinetics, safety, and tolerability of a rapid infusion of i.v. ibuprofen in healthy adults. *Am J Heal Pharm.* 2011;68(1):47–51.
31. Boase S, Miners JO. In vitro-in vivo correlations for drugs eliminated by glucuronidation: Investigations with the model substrate zidovudine. *Br J Clin Pharmacol.* 2002;54(5):493–503.
32. Davies NM. Clinical pharmacokinetics of ibuprofen. The first 30 years. *Clin Pharmacokinet.* 1998;34(2):101–54.
33. Cox SR. Effect of route of administration on the chiral inversion of (R)-ibuprofen. *Clin Pharmacol Ther.* 1988;43(2):146.
34. Cheng H, Rogers JD, Demetriades JL, Holland SD, Seibold JR, Depuy E. Pharmacokinetics and Bioinversion of Ibuprofen Enantiomers in Humans. Vol. 11, *Pharmaceutical Research.* 1994. p. 824–30.
35. Hall SD, Rudy AC, Knight PM, Brater DC. Lack of presystemic inversion of (R)- to (S)-ibuprofen in humans. *Clin Pharmacol Ther.* 1993;53(4):393–400.
36. Lockwood GF, Albert KS, Gillespie WR, Bole GG, Harkcom TM, Szpunar GJ, et al. Pharmacokinetics of ibuprofen in man. I. Free and total area/dose relationships. *Clin Pharmacol Ther.* 1983;34(1):97–103.
37. Abduljalil K, Pan X, Pansari A, Jamei M, Johnson TN. Preterm Physiologically Based Pharmacokinetic Model. Part II: Applications of the Model to Predict Drug Pharmacokinetics in the Preterm Population. *Clin Pharmacokinet.* 2019 Oct;
38. Calvier EAM, Krekels EHJ, Johnson TN, Tibboel D, Knibbe CAJ. Scaling Drug Clearance from Adults to the Young Children for Drugs Undergoing Hepatic Metabolism : A Simulation Study to Search for the Simplest Scaling Method. *AAPS J.* 2019;21(38).
39. Badée J, Qiu N, Collier AC, Takahashi RH, Forrest WF, Parrott N, et al. Characterization of the Ontogeny of Hepatic UDP-Glucuronosyltransferase Enzymes Based on Glucuronidation Activity Measured in Human Liver Microsomes. *J Clin Pharmacol.* 2019 Sep;59(S1):S42–55.
40. Strougo A, Yassen A, Monnereau C, Danhof M, Freijer J. Predicting the “First Dose in Children” of CYP3A-Metabolized Drugs : Evaluation of Scaling Approaches and Insights Into the CYP3A7-CYP3A4 Switch at Young Ages. *J Clin Pharmacol.* 2014;54(9):1006–15.
41. Edginton AN, Schmitt W, Willmann S. Development and evaluation of a generic physiologically based pharmacokinetic model for children. *Clin Pharmacokinet.* 2006;45(10):1013–34.
42. Stelova M, Holm R, Fotaki N, Reppas C, Vertzoni M. Successful extrapolation of paracetamol exposure from adults to infants after oral administration of a paediatric aqueous suspension is highly dependent on the study dosing conditions. *AAPS J.* 2020;22(126):1–17.
43. Hopkins CS, Underhill S, Booker PD. Pharmacokinetics of paracetamol after cardiac surgery. *Arch Dis Child.* 1990;65(9):971–6.

44. Walson PD, Halvorsen M, Edge J, Casavant MJ, Kelley MT. Pharmacokinetic Comparison of Acetaminophen Elixir Versus Suppositories in Vaccinated Infants (Aged 3 to 36 Months): A Single-Dose, Open-Label, Randomized, Parallel-Group Design. *Clin Ther*. 2013;35(2):135–40.
45. Stelova M, Holm R, Fotaki N, Reppas C, Vertzoni M. Factors affecting successful extrapolation of ibuprofen exposure from adults to paediatric populations after oral administration of a paediatric aqueous suspension. *AAPS J*. 2020; 22(146):1–17.
46. Brown RD, Wilson JT, Kearns GL, Eichler VF, Johnson VA, Bertrand KM. Single-dose pharmacokinetics of ibuprofen and acetaminophen in febrile children. *J Clin Pharmacol*. 1992;32:232–41.
47. Walson PD, Galletta G, Pharm D, Braden NT, Alexander L, Columbus BS. Ibuprofen, acetaminophen, and placebo treatment of febrile children. *Clin Pharmacol Ther*. 1989;46(1):9–17.